doi:10.1016/j.ymthe.2005.11.024

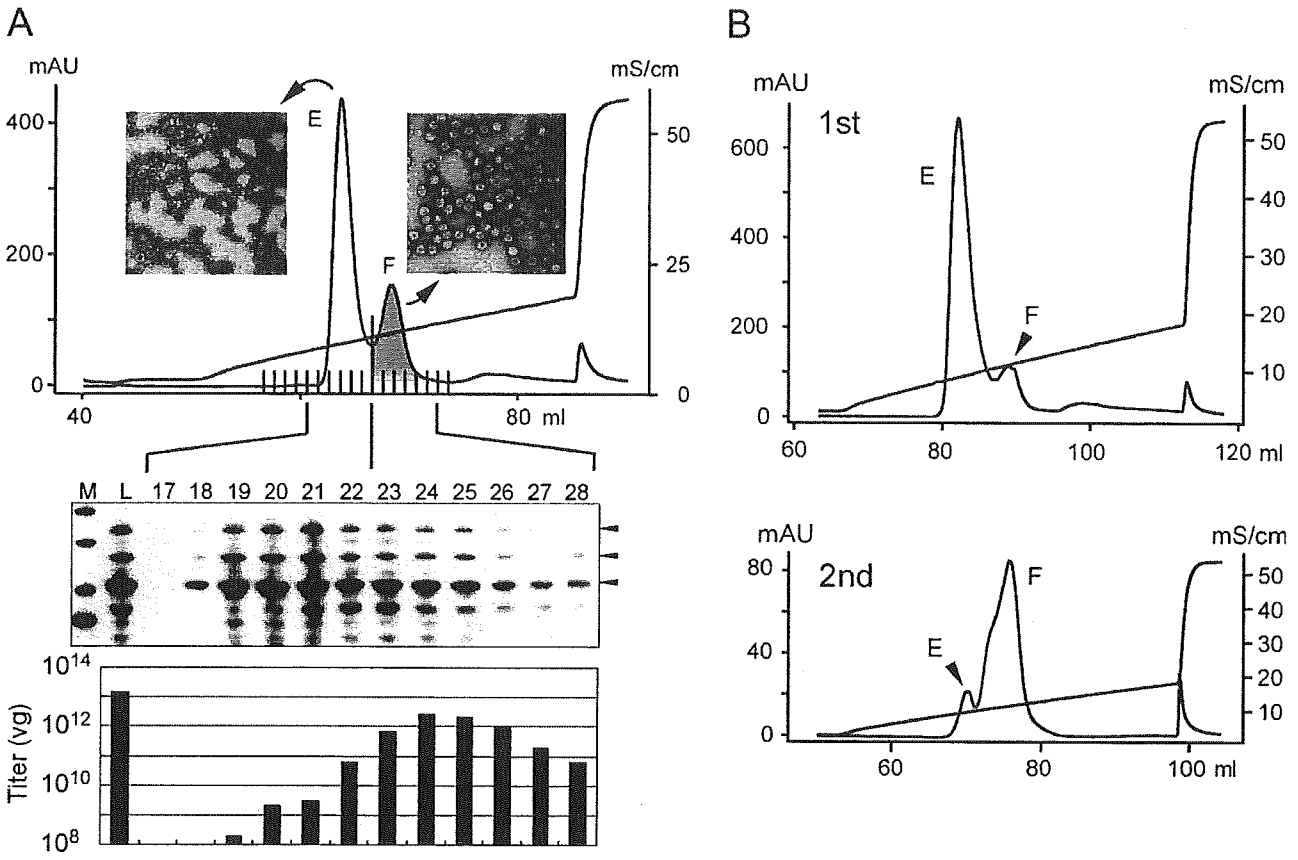

FIG. 2. (A) A representative chromatogram of a rAAV1-GFP preparation. Approximately 10^{13} vg of vector particles were generated and purified as described in the legend to Fig. 1 and finally loaded onto a 5-mm × 20-cm Tricorn column (Amersham Biosciences) packed with POROS HQ 10-μm matrix (Applied Biosystems) equilibrated with 25 mM *N*-methyldiethanolamine (pH 8.5) and 10 mM $[(CH_3)_4N]_2SO_4$. Bound viral particles were eluted with a 10–125 mM $[(CH_3)_4N]_2SO_4$ gradient over 38 ml at a flow rate of 0.5 ml/min. F and E indicate filled and empty particles, respectively. Electron microscopy of negatively stained samples from each peak is shown as an inset. After 1-ml fractionation samples were analyzed on a 4–12% NuPAGE gel (Invitrogen), the separated proteins were transferred to a Durapore membrane (Millipore, Bedford, MA, USA) and incubated with a rabbit polyclonal anti-type 5 VP antibody. After incubation with a secondary anti-rabbit immunoglobulin G labeled with horseradish peroxidase (Pierce, Milwaukee, WI, USA), chemiluminescent signals were detected using the SuperSignal West Pico Chemiluminescent substrate (Pierce) (middle). The fraction number is indicated above each lane. VP1, VP2, and VP3 capsid proteins are indicated by arrows. A sample from each fraction was also analyzed by real-time PCR to quantify the GFP vector DNA using a primer set specific to the CMV promoter, as previously described [15]. M, molecular weight standard; L, loaded sample. (B) An example of separation of rAAV1-GFP from empty particles by two runs of the high-resolution column chromatography. The first run was able to eliminate more than 90% of the contaminating empty capsids (E) from rAAV1-GFP (F). Reloading of the eluate from the first run further removed the contaminating empty particles.

We assessed the biological activity of the rAAV1-GFP isolated by column chromatography. We infected HEK293 cells with rAAV1-GFP samples, before or after chromatographic removal of empty particles, at the particle per cell numbers indicated (Fig. 3A). Seven days after transduction, we examined the cells under a fluorescence microscope. To quantify the GFP fluorescence, we also analyzed the cells by flow cytometry as described [13]. The analysis gave the percentage positive cells and the average GFP fluorescence, which refers to the average fluorescence intensity in the subpopulation of GFP-positive cells. The fluorescence volume represents a summation of GFP fluorescence within the subpopulation of GFP-positive cells, which was calculated to be equal to the fraction of GFP-positive cells in the sample population times the mean fluorescence intensity. When HEK293 cells were infected with either rAAV1-GFP at more than 10^4 vg per cell, both vectors transduced almost all the infected cells. However, the volume of GFP

TABLE 1: Recovery of rAAV1-GFP after removal of empty capsids

Preparations	Load	After 1st run (%)	After 2nd run (%)
#1	1.2×10^{13}	7.6×10^{12} (63.3)	5.0×10^{12} (41.7)
#2	3.3×10^{13}	2.4×10^{13} (72.7)	1.7×10^{13} (51.5)
#3	1.3×10^{13}	8.6×10^{12} (66.2)	6.8×10^{12} (52.3)

Number of rAAV1 particles was determined by real-time PCR. The percent recovery was calculated by dividing the number of rAAV1 particles loaded onto the first high resolution column by the number of rAAV particles recovered after chromatography.

Copyright © The American Society of Gene Therapy

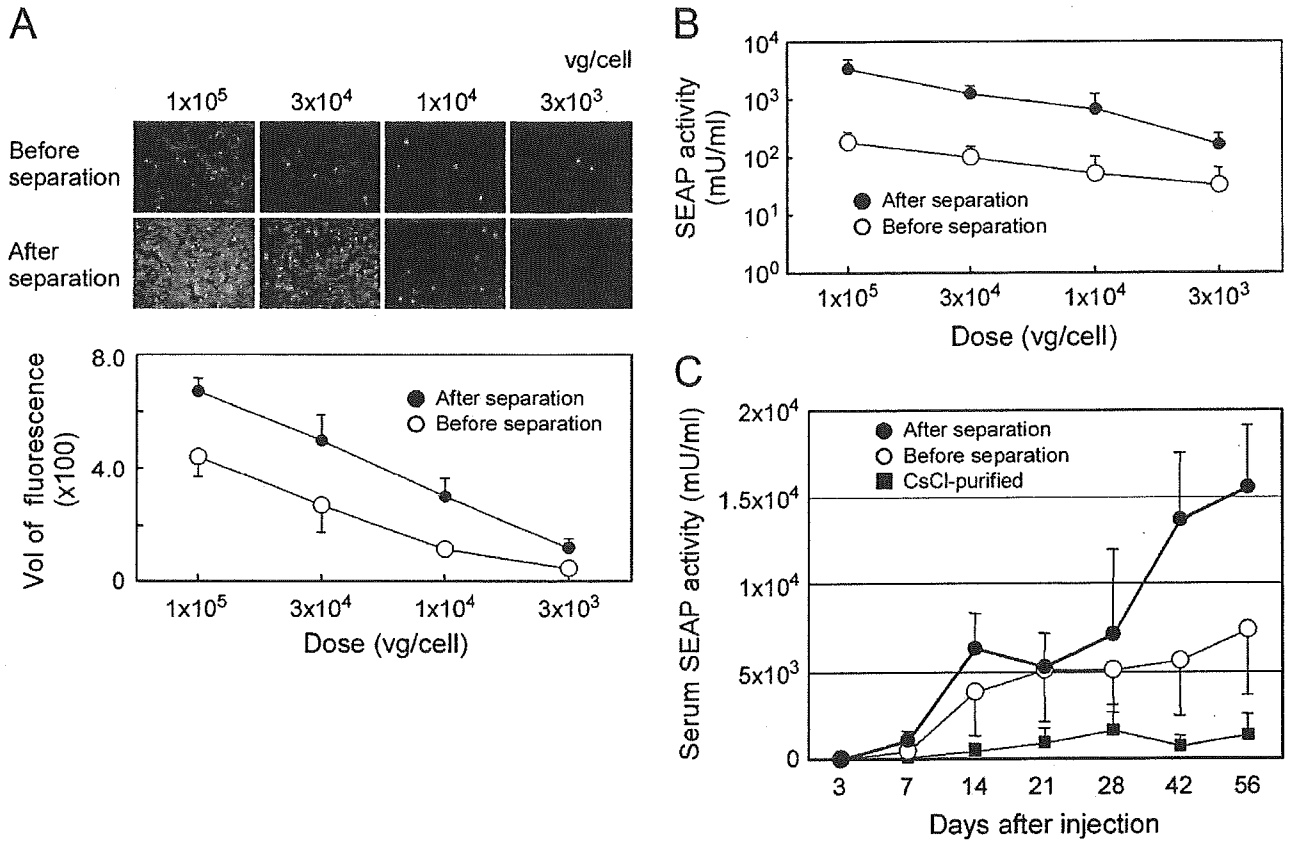

FIG. 3. (A) Transduction of HEK293 cells with rAAV1-GFP chromatographically separated from empty particles. 293 cells were infected with rAAV1-GFP before or after column chromatography intended to separate empty particles at the doses indicated. The GFP-expressing cells were analyzed by flow cytometry. The volume of GFP fluorescence was obtained by calculating (the fraction of GFP-positive cells) × (the average GFP fluorescence). Data represent means and standard deviation of experiments performed in triplicate. (B) The SEAP activity of the culture supernatant after infection of HEK293 cells with rAAV1-SEAP contaminated with or without empty particles. HEK293 cells were infected with type 1 SEAP vector before or after chromatographic removal of empty capsids at doses ranging from 1×10^5 through 3×10^3 vg per cell in triplicate. Results are expressed as means ± SD. (C) The serum SEAP levels after injection of rAAV1-SEAP into mouse muscles. A total of 10^{10} vg of rAAV1-SEAP particles before or after high-resolution chromatography or rAAV1-SEAP purified by CsCl ultracentrifugation was injected into mouse tibialis anterior muscles in triplicate and blood was taken from 3 through 56 days after injection.

fluorescence obtained by rAAV1-GFP separated from empty capsids was larger than that by rAAV contaminated with empty particles. We also infected HEK293 cells with rAAV1 expressing the human secreted alkaline phosphatase (SEAP). We excised the SEAP gene from pSEAP2-Basic (Clontech, Mountain View, CA, USA) with *Nru*I and *Sal*I and blunt-ended the resulting 1.8-kb fragment and inserted it between the type 2 ITRs. We used the resulting plasmid for transfection of HEK293 cells and purified rAAV1-SEAP as described above. We measured the SEAP activity in the culture supernatants 1 week after infection by using the SEAP Report Gene Assay (Roche Diagnostics, GmbH, Penzberh, Germany) according to the manufacturer's instructions. The rAAV1-SEAP separated from empty particles induced higher SEAP levels than rAAV1-SEAP contaminated with empty capsids at the doses tested (Fig. 3B). These results suggested that contaminating empty capsids interfered with the transduction of HEK293 cells by rAAV1.

To investigate the efficacy of rAAV1 *in vivo*, we injected rAAV1-SEAP (10^{10} vg) into mouse tibialis anterior muscles in triplicate. We used rAAV1-SEAP before chromatographic separation of empty capsids and CsCl-banded rAAV1-SEAP as controls. Fig. 3C shows the time course of the serum SEAP levels after the injection of SEAP vectors. rAAV1-SEAP purified by anion-exchange chromatography induced the highest levels of serum SEAP activity. The rAAV1-SEAP purified by column chromatography, but contaminated with empty particles, expressed lower levels of SEAP. CsCl-banded SEAP vector showed the lowest level, although the difference in the SEAP activity among the three groups was not statistically significant due to the small number of animals employed. The serum SEAP level at 56 days postinjection with the rAAV1 vector from which empty capsids were removed by chromatography was 10 times higher than that with the rAAV-SEAP from which empty capsids were excluded by CsCl ultracentrifugation, which may be due

Copyright © The American Society of Gene Therapy

doi:10.1016/j.ymthe.2005.11.024

to the impurity and/or the damage of CsCl-purified rAAV1 [14]. These results again indicated that the removal of empty particles from rAAV1 stocks by chromatography potentiated the SEAP expression in the muscles.

In summary, we report here a method for the selective removal of empty capsids from type 1 AAV vector. The chromatographic separation obtained pure rAAV1 stocks contaminated with less than 5% empty capsids. This method can remove empty capsids without the loss of the efficacy of rAAV1 and is easily scalable to a large volume. It will be useful for the purification of large quantities of rAAV1 for large-animal or human applications.

ACKNOWLEDGMENTS

We thank Robert Kotin (Laboratory of Biochemical Genetics, NIH) for his critical review of the manuscript. This work was supported in part by grants from the Ministry of Health, Welfare, and Labor of Japan and Grants-in-Aid for Scientific Research from the Ministry of Education, Science, Sports, and Technology of Japan and the High-Tech Research Center Project for private universities matching fund subsidy from the Ministry of Education, Science, Sports, and Technology of Japan.

RECEIVED FOR PUBLICATION SEPTEMBER 25, 2005; REVISED NOVEMBER 25, 2005; ACCEPTED NOVEMBER 28, 2005.

REFERENCES

1. Snyder, R. O. (1999). Adeno-associated virus-mediated gene delivery. *J. Gene Med.* **1:** 166–175.
2. Chao, H., Liu, Y., Rabinowitz, J., Li, C., Samulski, R. J., and Walsh, C. E. (2000). Several log increase in therapeutic transgene delivery by distinct adeno-associated viral serotype vectors. *Mol. Ther.* **2:** 619–623.
3. Kay, M. A., *et al.* (2000). Evidence for gene transfer and expression of factor IX in haemophilia B patients treated with an AAV vector. *Nat. Genet.* **24:** 257–261.
4. Arruda, V. R., *et al.* (2004). Safety and efficacy of factor IX gene transfer to skeletal muscle in murine and canine hemophilia B models by adeno-associated viral vector serotype 1. *Blood* **103:** 85–92.
5. Rabinowitz, J. E., *et al.* (2002). Cross-packaging of a single adeno-associated virus (AAV) type 2 vector genome into multiple AAV serotypes enables transduction with broad specificity. *J. Virol.* **76:** 791–801.
6. Dubielzig, R., King, J. A., Weger, S., Kern, A., and Kleinschmidt, J. A. (1999). Adeno-associated virus type 2 protein interactions: formation of pre-encapsidation complexes. *J. Virol.* **73:** 8989–8998.
7. Brument, N., *et al.* (2002). satile and scalable two-step ion-exchange chromatography process for the purification of recombinant adeno-associated virus serotypes-2 and -5. *Mol. Ther.* **6:** 678–686.
8. Clark, K. R., Liu, X., McGrath, J. P., and Johnson, P. R. (1999). Highly purified recombinant adeno-associated virus vectors are biologically active and free of detectable helper and wild-type viruses. *Hum. Gene Ther.* **10:** 1031–1039.
9. Zaiss, A. K., and Muruve, D. A. (2005). Immune responses to adeno-associated virus vectors. *Curr. Gene Ther.* **5:** 323–331.
10. Gao, G., *et al.* (2000). Purification of recombinant adeno-associated virus vectors by column chromatography and its performance in vivo. *Hum. Gene Ther.* **11:** 2079–2091.
11. Smith, R. H., Ding, C., and Kotin, R. M. (2003). Serum-free production and column purification of adeno-associated virus type 5. *J. Virol. Methods* **114:** 115–124.
12. Berns, K. I. (1996). Virology. In *Parvoviridae: the Viruses and Their Replication* (N. S. Fields, D. M. Knipe, P. M. Howley, R. M. Chanock, J. L. Melnick, T. P. Monath, B. Roizman Eds.), pp. 2173–2197. Lippincott–Raven, Philadelphia.
13. Soboleski, M. R., Oaks, J., and Halford, W. P. (2005). Green fluorescent protein is a quantitative reporter of gene expression in individual eukaryotic cells. *FASEB J.* **19:** 440–442.
14. Zolotukhin, S., *et al.* (1999). Recombinant adeno-associated virus purification using novel methods improves infectious titer and yield. *Gene Ther.* **6:** 973–985.
15. Urabe, M., Ding, C., and Kotin, R. M. (2002). Insect cells as a factory to produce adeno-associated virus type 2 vectors. *Hum. Gene Ther.* **13:** 1935–1943.

Copyright © The American Society of Gene Therapy

doi:10.1016/j.ymthe.2005.11.010

ARTICLE

A Histone Deacetylase Inhibitor Enhances Recombinant Adeno-associated Virus-Mediated Gene Expression in Tumor Cells

Takashi Okada,[1,*] Ryosuke Uchibori,[1] Mayumi Iwata-Okada,[2] Masafumi Takahashi,[3] Tatsuya Nomoto,[1] Mutsuko Nonaka-Sarukawa,[1] Takayuki Ito,[1] Yuhe Liu,[1] Hiroaki Mizukami,[1] Akihiro Kume,[1] Eiji Kobayashi,[3] and Keiya Ozawa[1,2]

[1]*Division of Genetic Therapeutics,* [3]*Division of Organ Replacement Research, Center for Molecular Medicine, and* [2]*Division of Hematology, Department of Medicine, Jichi Medical School, Tochigi 329-0498, Japan*

**To whom correspondence and reprint requests should be addressed at the Division of Genetic Therapeutics, Center for Molecular Medicine, Jichi Medical School, 3311-1 Yakushiji, Minami-Kawachi, Tochigi 329-0498, Japan. Fax: +81 285 44 8675. E-mail: tokada@jichi.ac.jp.*

The transduction of cancer cells using recombinant adeno-associated virus (rAAV) occurs with low efficiency, which limits its utility in cancer gene therapy. We have previously sought to enhance rAAV-mediated transduction of cancer cells by applying DNA-damaging stresses. In this study, we examined the effects of the histone deacetylase inhibitor FR901228 on tumor transduction mediated by rAAV types 2 and 5. FR901228 treatment significantly improved the expression of the transgene in four cancer cell lines. The cell surface levels of alpha v integrin, FGF-R1, and PDGF-R were modestly enhanced by the presence of FR901228. These results suggest that the superior transduction induced by the HDAC inhibitor was due to an enhancement of transgene expression rather than increased viral entry. Furthermore, we characterized the association of the acetylated histone H3 in the episomal AAV vector genome by using the chromatin immunoprecipitation assay. The results suggest that the superior transduction may be related to the proposed histone-associated chromatin form of the rAAV concatemer in transduced cells. In the analysis with subcutaneous tumor models, strong enhancement of the transgene expression as well as therapeutic effect was confirmed *in vivo*. The use of this HDAC inhibitor may enhance the utility of rAAV-mediated transduction strategies for cancer gene therapy.

Key Words: histone deacetylase inhibitor, AAV vector, cancer

INTRODUCTION

Recombinant adeno-associated virus (rAAV) has been of considerable interest to developers of clinical gene therapies [1,2]. This is because, unlike adenoviruses, the introduction of AAV vectors has not been associated with significant inflammation either experimentally or clinically [3]. Furthermore, diseases associated with AAV have not been found in human or animal populations. However, the transduction of cancer cells using rAAV occurs with very low efficiency, which limits its utility in gene therapy. Consequently, we have sought to enhance rAAV-mediated transduction of cancer cells by applying DNA-damaging stresses such as γ-rays or anticancer agents [4–6].

An alternative approach to improving the rAAV-mediated transduction of tumor cells may be to enhance transcription in the target cells. One technique to bring about this event may be to apply a histone deacetylase (HDAC) inhibitor, since HDAC inhibitors are known to regulate the transcription of various genes. Significantly, an HDAC inhibitor increases adenovirus-mediated transduction of cancer cell lines because it enhances the levels of the viral receptor on the cell surface [7]. On the other hand, the effects of HDAC inhibitors on rAAV-mediated transduction of tumor cells have not yet been fully elucidated. Treatment with an HDAC inhibitor causes gene expression from a silenced rAAV genome that has been integrated into the host's genome to recover [8]. However, rAAV exists mostly as an extrachromosomal genome rather than as an integrated genome, and this extrachromosomal form is the primary source of rAAV-mediated gene expression [9]. Therefore, the HDAC inhibitor-mediated recovery of expression from the integrated and silenced genome does not reflect a typical situation of rAAV-mediated transduction. Whereas no

Copyright © The American Society of Gene Therapy
1525-0016/$30.00

doi:10.1016/j.ymthe.2005.11.010

clear mechanism has been determined for the effect on the episomal vector-mediated expression, the histone deacetylase inhibitor should also contribute to the enhanced transcription before integration occurs.

Here we show that HDAC inhibitors markedly enhance the transgene expression immediately after rAAV-mediated transduction of tumor cells *in vitro* as well as *in vivo*. Our data also suggest that the vector genome in the cells is in the histone-associated chromatin form, which is capable of superior transcription. HDAC inhibitors may improve tumor cell transduction by enhancing the acetylation of the histone-associated chromatin of the rAAV genome.

RESULTS

Effects of FR901228 Treatment on the Transduction of U251MG Cells with rAAV

To analyze whether an HDAC inhibitor can also improve rAAV-mediated gene expression soon after the infection,

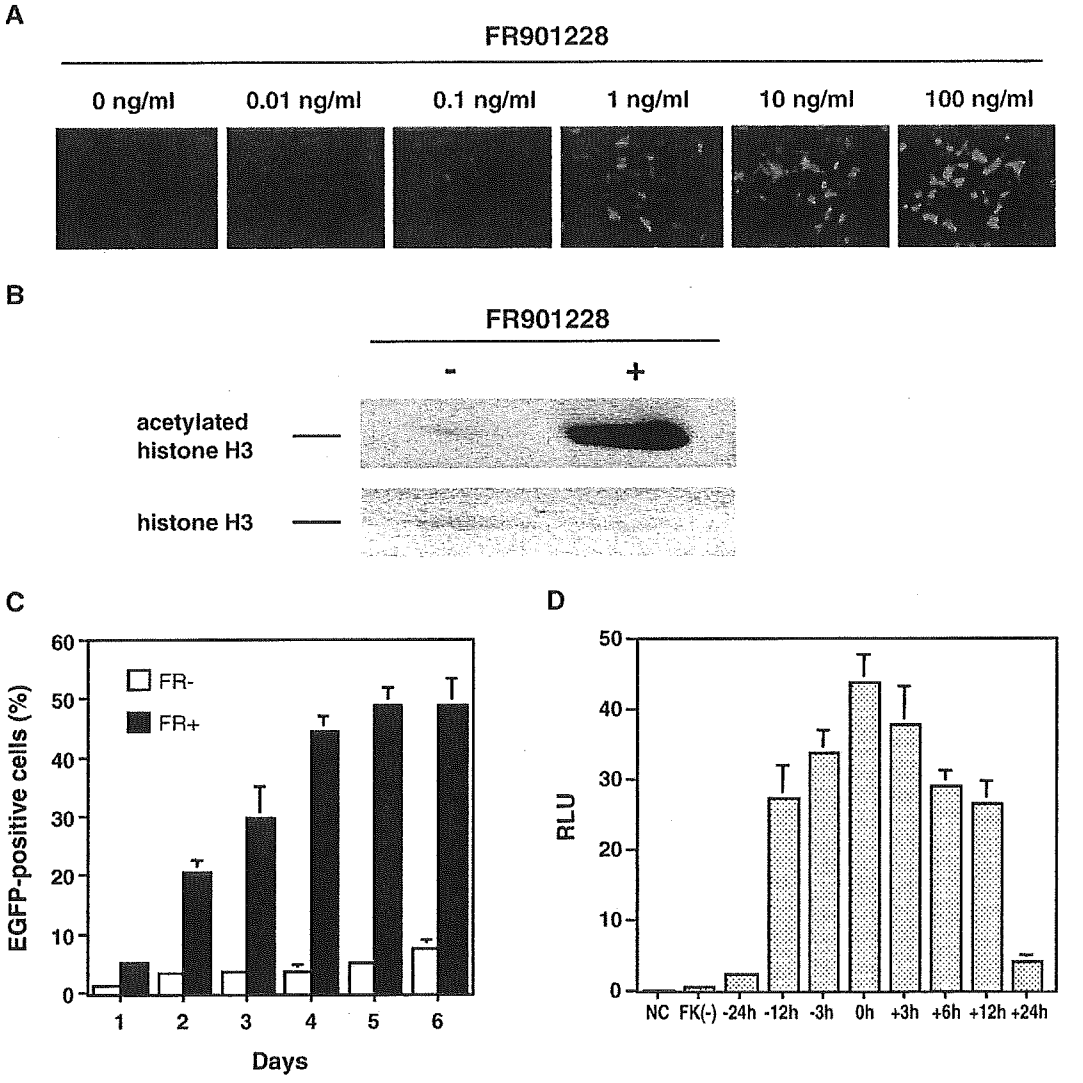

FIG. 1. (A) Effects of FR901228 treatment on the transduction of U251MG cells with rAAV. U251MG cells were infected with 1×10^4 genome copies/cell of AAV2EGFP in the presence of various concentrations of FR901228. EGFP expression was observed 24 h after infection. (B) Detection of the histone acetylation in U251MG cells caused by FR901228 treatment. Cells were incubated in the presence or absence of FR901228 for 24 h. The levels of acetylated histone H3 and histone H3 were determined by Western blot analysis. Histone H3 serves as a loading control. (C) The percentage of EGFP-positive cells at various time points after transduction with AAV2EGFP in the presence (FR+) or absence (FR−) of 1 ng/ml FR901228 was determined by FACS. Cells were infected with AAV2EGFP at 1×10^3 genome copies/cell. The data shown are the means and standard deviations of three independent experiments. (D) The kinetics of the effect on the FR901228-assisted transduction of U251MG cells. Cells were treated with FR901228 at various time points around the transduction with rAAV expressing luciferase as indicated. Luciferase assay was performed on the luminometer 48 h after the transduction.

Copyright © The American Society of Gene Therapy

we transduced U-251MG human glioma cells with EGFP-expressing rAAV (AAV2EGFP) in the presence of the HDAC inhibitor FR901228. We found that FR901228 treatment improved the AAV2EGFP-mediated gene expression in a dose-dependent manner early after the infection (Fig. 1A). The fact that FR901228 also enhanced the acetylation of the histones in the cells was confirmed by Western blot analysis (Fig. 1B). To assess when gene expression was maximal, we transduced U251MG cells with AAV2EGFP in the presence or absence of 1 ng/ml FR901228 and assessed EGFP expression at various time points after transduction (Fig. 1C). This revealed that the enhancement of gene expression depended on the incubation period and required 4 days before the expression reach a plateau. To analyze the kinetics of the effect on the FR901228-assisted transduction of U251MG cells, cells were treated with FR901228 at various time points around the transduction with luciferase-expressing rAAV type 2 (AAV2-Luc) (Fig. 1D). As a result, the transduction efficiency peaked when cells were treated with FR901228 at the time of virus transduction.

TABLE 1: Relative expression of FGF-R1 and PDGF-R in U251MG cells treated with recombinant AAV alone (1×10^4 genome copies/cell) or together with FR901228 (0.3 or 3 ng/ml) for 24 h as analyzed by quantitative PCR

FR901228 (ng/ml)	$2^{\text{correctedΔCt (GAPDH – target)}}$	
	FGF-R1	PDGF-Rα
0	1.00	1.00
0.3	1.28	1.77
3	1.60	2.30

The relative expression of the target mRNA was determined as the ratio of the expression in U251MG cells treated with recombinant AAV and FR901228 to that in U251MG cells treated with recombinant AAV alone. Data are means ($n = 5$).

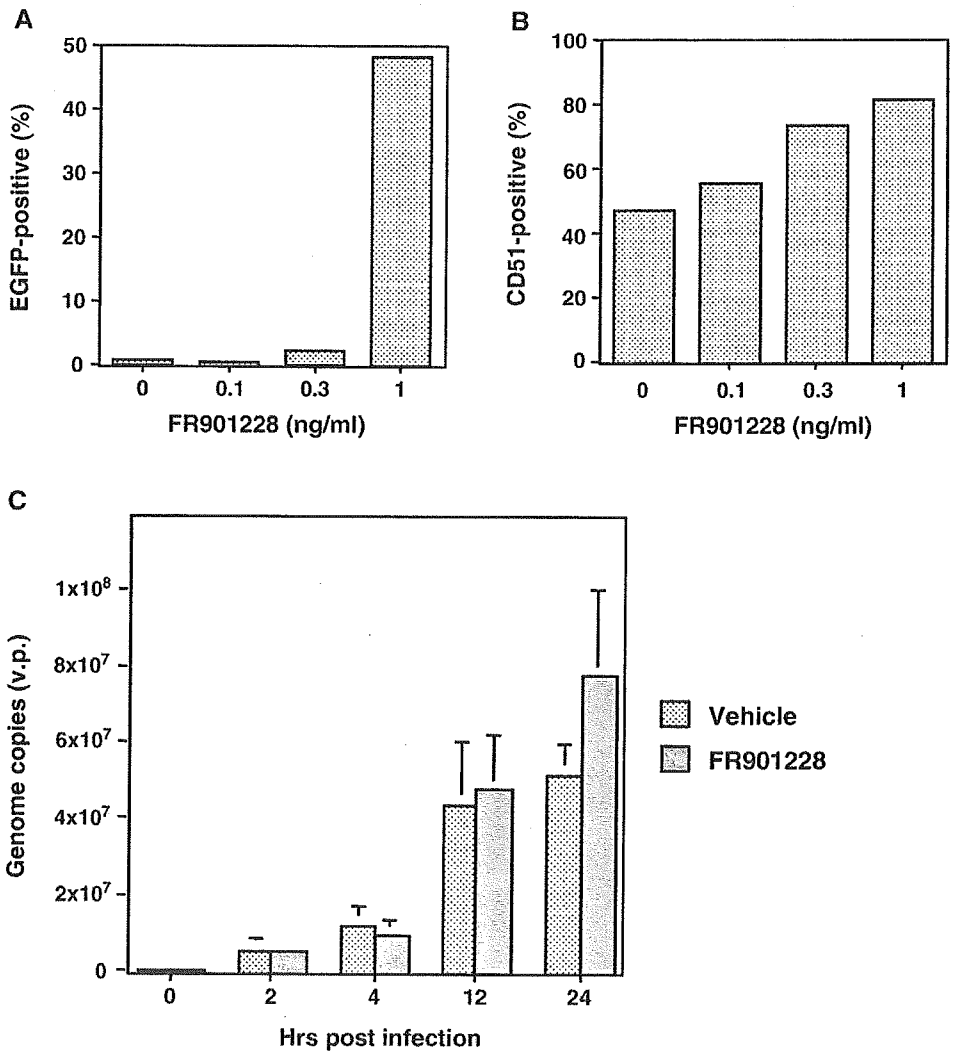

FIG. 2. (A) Percentage of EGFP-positive U251MG cells after transduction with 1×10^4 genome copies/cell of AAV2EGFP in the presence of various concentrations of FR901228. The cells were analyzed 24 h after the transduction for EGFP expression by FACS. The data shown are the average percentages of EGFP-positive cells after three independent transductions. (B) Integrin expression in transduced cells is only modestly enhanced by FR901228 treatment. The cells were stained 24 h after the transduction with monoclonal antibodies to CD51 (integrin v chain, clone 13C2) and analyzed by FACS. The data shown are the average percentages of positive cells after three independent transductions. (C) Transgene copy number in U251MG cells transduced with 1×10^4 genome copies/cell of AAV2EGFP in the presence of 1 ng/ml FR901228. The copy number of the transgene was estimated by real-time PCR at 0, 2, 4, 12, and 24 h after the rAAV infection.

Copyright © The American Society of Gene Therapy

doi:10.1016/j.ymthe.2005.11.010

Effects on Receptor Expression and Viral Entry

To determine if FR901228 acted by enhancing the entry of rAAV, we infected U251MG cells with AAV2EGFP in the presence of various concentrations of FR901228 and then analyzed the EGFP and alpha v integrin levels in the cells by fluorescence-activated cell sorting (FACS). This analysis showed that 24 h after AAV2EGFP infection with 1 ng/ml FR901228, 48% of the U251MG cells were EGFP-positive, whereas at lower concentrations of FR901228 only very few cells were EGFP-positive (Fig. 2A). However, this FR901228 concentration range (0.3–1 ng/ml) only modestly enhanced the levels of AAV2 coreceptor, alpha v integrin (Fig. 2B). In addition, when we estimated the amount of the rAAV genome in the transduced cells by real-time quantitative PCR analysis, we found that FR901228 treatment did not significantly affect the copy number of the rAAV (Fig. 2C). Furthermore, we also estimated the effect of FR901228 on the expression of coreceptors for the AAV. FR901228 moderately

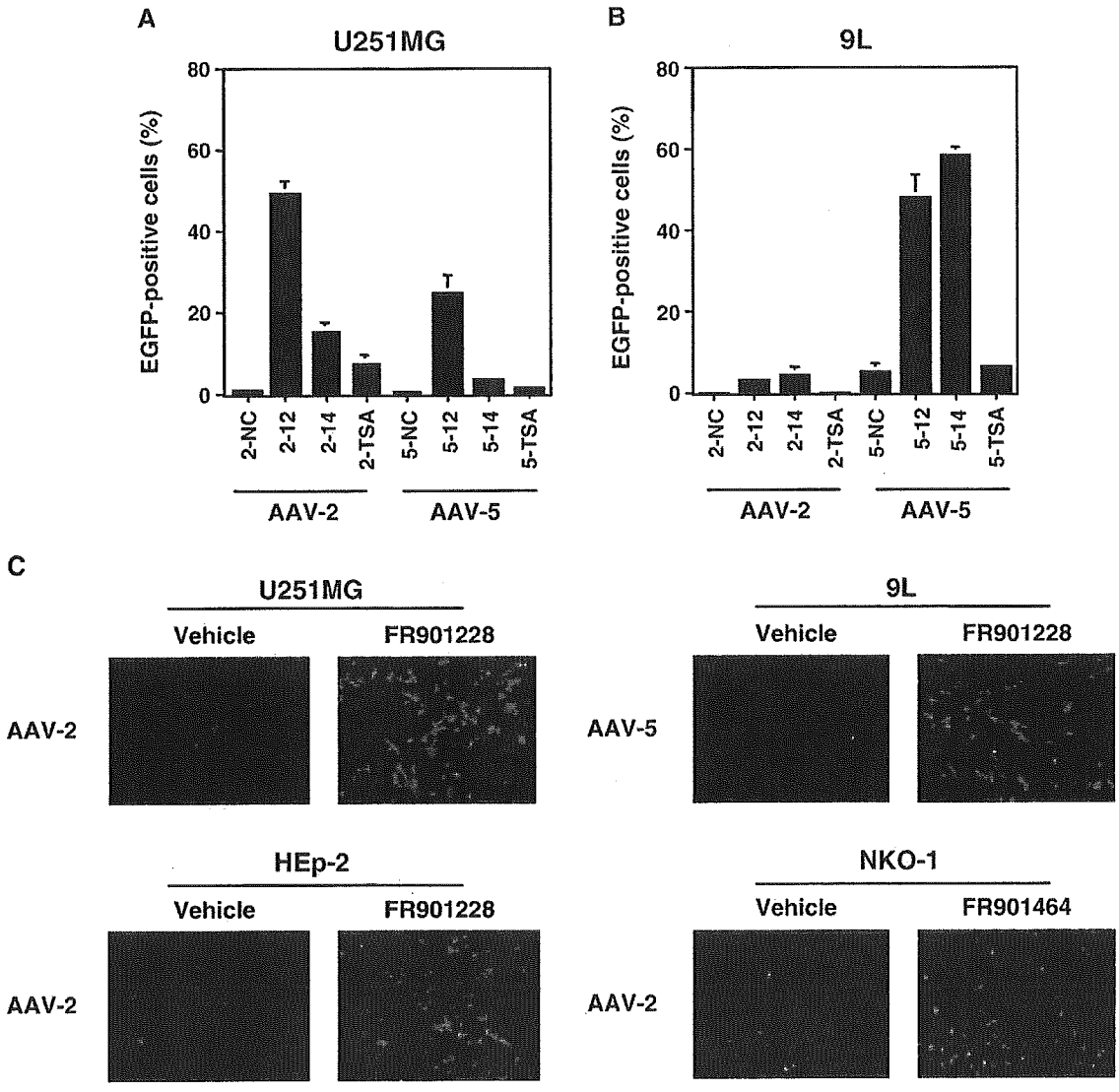

FIG. 3. (A, B) EGFP expression by AAV2EGFP and AAV5EGFP differs depending on the tumor cell being transduced. U251MG or 9L cells were infected with 1 × 10^4 genome copies/cell of AAV2EGFP (2) or AAV5EGFP (5) in the presence of vehicle (NC) or 1 ng/ml of various HDAC inhibitors, FR901228 (12), FR901464 (14), or TSA. The cells were analyzed by FACS 24 h after the infection. The data show the average percentages of EGFP-positive cells after three independent transductions + SD. (C) Representative data of the enhanced transgene expression by HDAC inhibitors in various cell lines infected with AAV vectors. Twenty-four hours after the AAV2EGFP or AAV5EGFP infection at 1 × 10^4 genome copies/cell with 1 ng/ml of the FR901228 or FR901464, cells were examined under the fluorescence microscope.

Copyright © The American Society of Gene Therapy

increased mRNA levels of fibroblast growth factor receptor 1 (FGF-R1) and platelet-derived growth factor receptor (PDGF-R), although the augmentation was not enough to explain the drastic increase of the expression (Table 1).

Transduction of Tumor Cells with AAV Vectors Derived from Distinct Serotypes

Type 2 and type 5 rAAV differed from each other in the efficiency of their transduction of U251MG and the 9L glioma cells. Although FR901228 and other HDAC inhibitors (FR901464 or trichostatin A (TSA)) remarkably enhanced the transduction of both rAAVs in general, AAV2EGFP-mediated transduction of U251MG cells was more efficient than AAV5EGFP-mediated transduction while AAV5EGFP-mediated transduction of 9L cells was better than AAV2EGFP-mediated transduction (Figs. 3A and 3B). FR901228 and FR901464 also had promoting effects on AAV2EGFP- and AAV5EGFP-mediated transduction of the head and neck cancer cell lines HEp-2 and NKO-1 (Fig. 3C).

Chromatin Modification with FR901228

We characterized chromatin composition of the episomal AAV vector genome by using the chromatin immunoprecipitation (ChIP) assay. ChIP is a technique to test for the presence of certain DNA-binding proteins that might modulate chromatin structure and/or transcriptional characteristics of the specific region of DNA with which they are associated. We made use of polyclonal antibodies generated against histone H3 as well as acetylated histone H3, which have been linked to chromatin modification and regulation of transcription. The primers for the CMV promoter region in the AAV vector genome gave a higher level of PCR product when used on templates from FR901228-treated cells compared to those from cells without FR901228 treatment. Higher levels of acetylated histone H3 were found on the CMV promoter region of the AAV vector versus the GAPDH promoter region of the cellular DNA (Table 2A). In contrast, enrichment of acetylated histone H3-associated DNA was not significant on plasmid vector genome irrespective of the presence of the ITR (Table 2B).

FR901228-Assisted Enhancement of Tumor Transduction *in Vivo*

In the analysis using optical bioluminescence imaging of the subcutaneous tumors, we confirmed drastic enhancement of the luciferase gene expression *in vivo* (Fig. 4A). The signal intensity in animals treated with FR901228 (n = 5, [1.5 ± 0.9] × 10^6 photons/s/cm^2/sr) was 37.4-fold higher than in control animals (n = 3, [4.0 ± 2.4] × 10^4 photons/s/cm^2/sr). A subcutaneous

TABLE 2: PCR amplification of immunoprecipitated DNA

(A) Chromatin composition of episomal AAV vector genome was characterized by using the chromatin immunoprecipitation assay

Ab of interest	FR901228	$2^{\text{correctedΔCt (GAPDHprom – CMVprom)}}$
Rabbit IgG	–	<0.001
Rabbit IgG	+	<0.001
Anti-histone H3	–	1.0 ± 1.8
Anti-histone H3	+	7.3 ± 1.4
Anti-acetyl histone H3	–	1.0 ± 0.4] < 0.0001
Anti-acetyl histone H3	+	22.0 ± 0.8]

(B) Cells were transfected with a plasmid harboring the EGFP expression cassette under the CMV promoter (pEGFP) or a plasmid carrying an identical EGFP expression cassette flanked by ITR regions (pITR-EGFP)

Plasmid	Ab of interest	FR901228	$2^{\text{correctedΔCt (GAPDHprom – CMVprom)}}$
pEGFP	Rabbit IgG	–	<0.001
	Rabbit IgG	+	<0.001
	Anti-acetyl histone H3	–	1.0
	Anti-acetyl histone H3	+	1.3
pITR-EGFP	Rabbit IgG	–	<0.001
	Rabbit IgG	+	<0.001
	Anti-acetyl histone H3	–	1.0
	Anti-acetyl histone H3	+	1.2

U251MG cells were transduced with AAV vector at 1 × 10^4 genome copies/cell in the presence or absence of 1 ng/ml FR901228. Twenty-four hours after the transduction, chromatin proteins of interest were cross-linked to DNA by formaldehyde. Shared DNA was immunoprecipitated with histone H3 antibody or acetylated histone H3 antibody to enrich for the CMV promoter region or GAPDH promoter region. Relative differences in the levels of immunoprecipitated DNA, which are reflective of the levels of the chromatin protein of interest occupying a particular island, between different promoter regions and cell treatment with FR901228 were quantified by quantitative PCR.

Copyright © The American Society of Gene Therapy

doi:10.1016/j.ymthe.2005.11.010

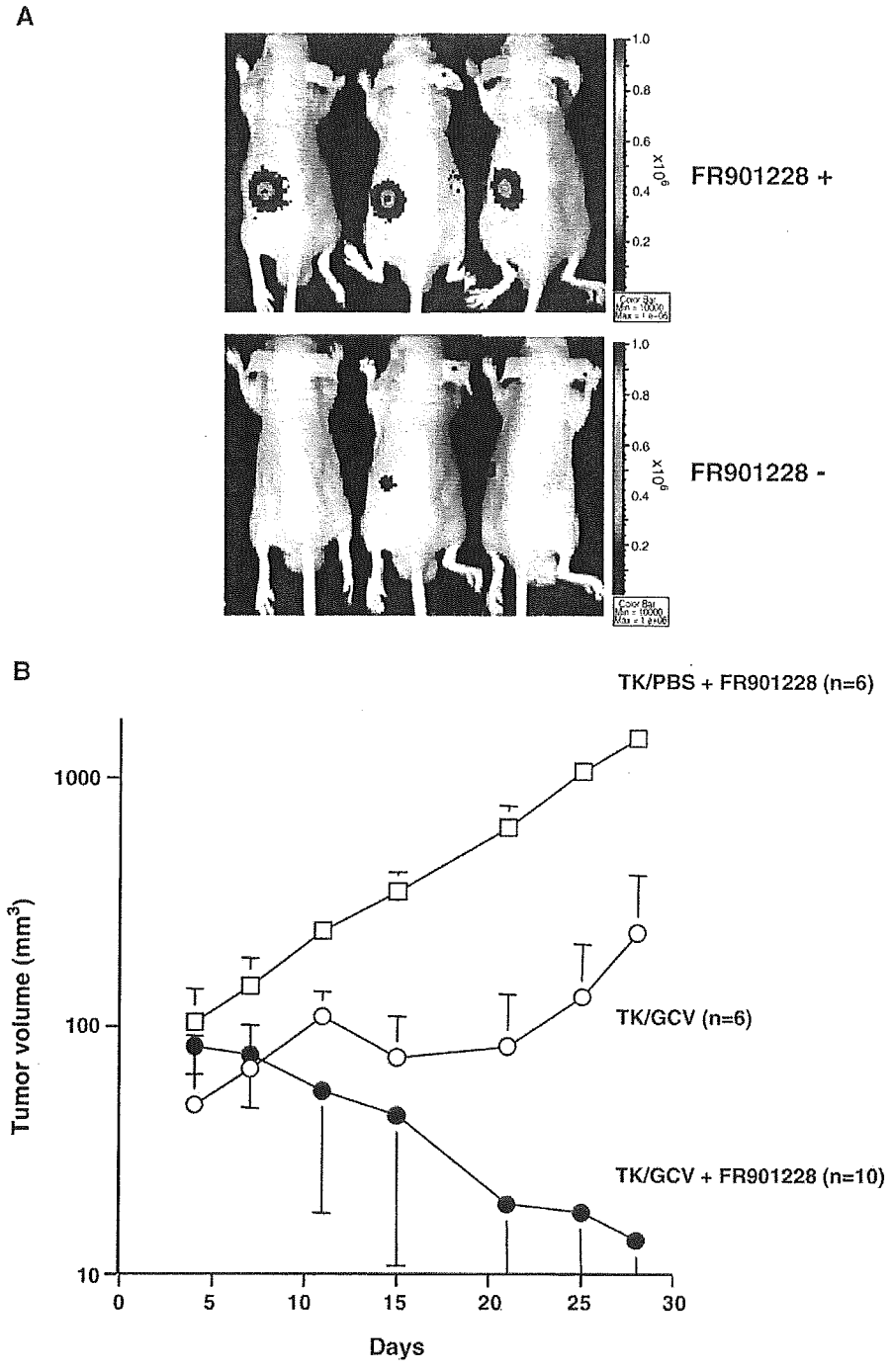

FIG. 4. (A) FR901228-assisted enhancement of tumor transduction *in vivo*. U251MG cells were mixed with PBS (FR901228−, n = 3) or transduced with a recombinant AAV2 expressing luciferase (AAV2Luc) at 1×10^4 genome copies/cell for 1 h (FR901228+, $n = 5$), and then 3×10^6 of the transduced cells in 100 μl PBS were inoculated subcutaneously into the BALB/c mice along with the intraperitoneal injection of FR901228 at 1 mg/kg. Twenty-four hours after administration of the FR901228, optical bioluminescence imaging was performed using the CCD camera. (B) The effects of FR901228 on the rAAV-mediated transduction for 9L tumor elimination *in vivo*. Cells were transduced with AAV5TK at 1×10^4 genome copies/cell for 1 h, and then 3×10^6 of the transduced cells in 100 μl PBS containing 25% (v/v) basement membrane matrix were inoculated subcutaneously into the BALB/c mice. The tumor-bearing animals received intraperitoneal injection of FR901228 at 3 mg/kg (group 1, n = 6; group 3, n = 10) or PBS (group 2, n = 6). The animals were also exposed to ganciclovir (GCV) at 100 mg/kg per day (groups 2 and 3) or PBS (group 1) for 14 consecutive days by intraperitoneal placement of the miniosmotic pumps.

tumor model with athymic nude mice demonstrated that the combination of AAV-mediated transduction for HSV-*tk*/GCV therapy and FR901228 treatment (n = 10) resulted in statistically significant reduction of tumor growth relative to HSV-*tk*/GCV therapy without FR901228 treatment (unpaired t test, $P < 0.05$, n = 6; Fig. 4B). When the tumor-bearing animals were treated with GCV and FR901228, 8 of 10 tumors were eliminated at 4 weeks after transduction.

Discussion

HDAC inhibitors significantly improved the expression of the transgene in cancer cells. The enhancement of the coreceptor level was modest and copy number of the

Copyright © The American Society of Gene Therapy

rAAV in the transduced cells was also modestly affected by the FR901228 treatment. Furthermore, association of the acetylated histone H3 in the episomal AAV vector genome was demonstrated by using the chromatin immunoprecipitation assay. In the analysis with the subcutaneous tumor models, strong enhancement of the transgene expression as well as therapeutic effect was confirmed *in vivo*.

Treatment with an HDAC inhibitor is known to cause the recovery of the gene expression of a rAAV vector genome that has been integrated and silenced after long-term selection [8]. However, rAAV occurs mostly as extrachromosomal genomes rather than as integrated genomes, and these extrachromosomal forms are the primary source of rAAV-mediated gene expression early after transduction [9]. There has been no direct investigation of the effects of HDAC inhibitors on the rAAV-mediated transient gene expression. We examined whether the HDAC inhibitor could contribute to the enhanced transcription before integration occurs.

FR901228 treatment significantly improved the transient expression of the transgene in four cancer cell lines. The FR901228 treatment improved the rAAV-mediated gene transfer in a dose-dependent manner, and the highest enhancement was observed in the U251MG cells with AAV2EGFP. In the U251MG cells, the cell surface levels of alpha v integrin, FGF-R1, and PDGF-R were only modestly enhanced by the presence of FR901228. These observations contrast with a previous report that suggested that FR901228 enhanced adenovirus transduction by increasing CAR and v integrin RNA levels, thereby enhancing viral entry [7]. However, their study did not demonstrate that these increased RNA levels were associated with increased protein levels or kinetics. In our study, a kinetic analysis of the effect on the FR901228-assisted AAV-mediated transduction of U251MG cells showed that the transduction efficiency peaked when cells were treated with FR901228 at the time of transduction. This is in sharp contrast to the case of the effect of FR901228 on the enhanced adenovirus-mediated transduction. Since enhanced viral entry into the cell is a primary function of FR901228 regarding improved adenovirus transduction, transduction efficiency of the adenovirus was preferentially enhanced when the cells were pretreated with FR901228 before transduction [10].

Interestingly, we observed that type 2 and type 5 rAAV differed from each other in the efficiency of their transduction of the U251MG and 9L cells. The differences in the transduction efficiency of the AAV vectors derived from distinct serotypes may be due to the fact that each AAV serotype recognizes a different receptor and that different cell types may express different levels of these receptors. Type 2 AAV uses the cell surface heparan sulfate proteoglycan (HSPG) as a receptor [11]. However, cell surface expression of HSPG alone is insufficient for type 2 AAV infection and FGF-R1 is also required as a coreceptor for successful viral entry into the host cell [12]. Type 5 AAV transduction requires 2,3-linked sialic acid [13] as well as PDGF-R [14] for efficient binding and transduction. These observations indicate that optimized expression of a transgene borne by rAAV will require the careful selection of the appropriate vector serotype with respect to the target cell.

Our data also suggest that the use of FR901228 in combination with AAV vector infection may improve viral entry into the cells, but also requires additional mechanisms to benefit the target cells for the efficient transduction. Association of the acetylated histone H3 in the episomal AAV vector genome was characterized by using the chromatin immunoprecipitation assay. Characterization of the chromatin modification in the rAAV genome with FR901228 suggested that improved expression of the transgene depends on the chromatin state of the AAV genome in the infected cells rather than viral entry. These results suggest that the superior transduction induced by HDAC inhibitor treatment is actually due to an enhancement of transgene expression associated with chromatin modification rather than to increased viral entry. Thus, epigenetic regulatory mechanisms may be involved in the HDAC inhibitor-mediated improvement of the transduction of cancer cells with rAAV. The rAAV concatemer may need to be present in a histone-associated chromatin form in the cells before efficient transgene expression can occur.

Our study suggests that the improved rAAV-mediated transduction induced by HDAC inhibitor was due to an enhancement of transgene expression rather than increased viral entry. This phenomenon may be related to the proposed histone-associated chromatin form of the rAAV concatemer in transduced cells. The depsipeptide fermentation product FR901228 is currently being tested in clinical trials as an anti-cancer drug. Therefore, to utilize such a compound to assist rAAV-mediated cancer gene therapy is theoretically and practically reasonable. The use of HDAC inhibitors may enhance the utility of rAAV-mediated transduction strategies for future clinical investigation.

Materials and Methods

Recombinant AAV production. The EGFP expression cassette driven by the CMV promoter was ligated into pAAVLacZ [15] and pAAV5-RNL [16] to form the proviral plasmids pAAV2EGFP and pAAV5EGFP. rAAV types 2 and 5 that express the EGFP gene (AAV2EGFP and AAV5EGFP) were generated using the proviral plasmids. The luciferase expression cassette driven by the CMV promoter in pLNCL [17] was cloned into pAAVLacZ to create pAAV2Luc. A rAAV type 2 that expresses the luciferase gene (AAV2Luc) was generated using pAAV2Luc. Likewise, the HSV-*tk* cDNA contained in the pAVS6TK [18] was subcloned into pAAV5-RNL to create pAAV5TK. A rAAV type 5 that expresses the HSV-*tk* gene driven by the CMV promoter (AAV5TK) was generated using pAAV5TK. Transfection of 293 cells with the proviral plasmid, AAV helper plasmid pAAV2H [15] or pAAV5H [16], and adenoviral helper plasmid pAdeno was performed according to the previously described protocol [19] associated with an

Copyright © The American Society of Gene Therapy

doi:10.1016/j.ymthe.2005.11.010

active gassing [20]. The physical titer of the viral stock was determined by dot-blot hybridization with plasmid standards.

HDAC inhibitors. The HDAC inhibitor FR901228 (obtained from Fujisawa Pharmaceutical Co., Ltd.) is a depsipeptide fermentation product from *Chromobacterium violaceum* [21]. FR901228 strongly inhibits the proliferation of tumor cells by arresting cell cycle transition and is now being tested in clinical trials [22]. FR901464 (obtained from Fujisawa Pharmaceutical Co., Ltd.) and TSA (Sigma–Aldrich Corp., St. Louis, MO, USA) are also prepared as HDAC inhibitors [21].

Cells and culture. The malignant human glioma cell line U251MG, the malignant rat glioma cell line 9L, the laryngeal epidermoid carcinoma cell line HEp-2, and the human maxillary sinus cancer cell line NKO-1 were used in this study. Cells were cultured in Dulbecco's modified Eagle medium (D-MEM) supplemented with 10% fetal bovine serum (FBS), 100 units/ml penicillin, and 100 μg/ml streptomycin at 37°C, 5% CO_2. Human embryonic kidney 293 cells were cultured with D-MEM:F12 (1:1 mixture) supplemented with 10% FBS, 100 units/ml penicillin, and 100 μg/ml streptomycin at 37°C, 5% CO_2. Luciferase assay was performed on the luminometer (Fluoroskan Ascent FL, Thermo Labsystems, Beverly, MA, USA) using the Bright-Glo Reagent kit (Promega, Madison, WI, USA).

FACS analysis. Approximately 5×10^4 cells were analyzed on the FACScan (Becton–Dickinson, San Jose, CA, USA) with CellQuest software (Becton–Dickinson). Cells were incubated with a PE-labeled monoclonal antibody (13C2) specific for human integrin v chain (CD51; Cymbus Biotechnology Ltd., Chandlers Ford, UK) for 30 min on ice. The 7-aminoactinomycin-D (Via-Probe; Pharmingen, San Diego, CA, USA)-negative cell fraction, which contains the viable cells, was used to detect EGFP- and/or PE-positive cells.

Western blot analysis. Detection of histone acetylation by FR901228 in U251MG cells was performed as described [7]. Western blot analysis of the cells incubated in the presence or absence of FR901228 for 24 h was performed using either a rabbit polyclonal antibody against histone H3 or one against acetylated histone H3 (Upstate Biotechnology, Lake Placid, NY, USA) diluted 1:2000 in 5% milk. The probed membrane was incubated with an anti-rabbit immunoglobulin horseradish peroxidase-linked antibody and developed by ECL Western blotting detection reagents (Amersham Pharmacia Biotech, Piscataway, NJ, USA).

Determination of transgene copy number. Tumor cells were infected with 1×10^4 genome copies/cell of rAAV in the presence of FR901228. The high-molecular-weight DNA was extracted from the cells (DNA Extraction Kit; Qiagen, Inc., Hilden, Germany) 0, 2, 4, 12, and 24 h later. The copy numbers were determined by quantitative PCR analysis of 100 ng of the DNA by using an ABI Prism 7700 sequence detection system (Applied Biosystems, Foster City, CA, USA) as described in the supplementary information.

mRNA analysis of coreceptors for the AAV. U251MG cells were incubated with recombinant AAV either alone (1×10^4 genome copies/cell) or together with FR901228 (0.3 or 3 ng/ml) for 24 h. mRNA was isolated from the cell culture using an RNeasy mini kit (Qiagen) and reverse-transcribed into a single-stranded cDNA using the SuperScript Preamplification System (Invitrogen, Carlsbad, CA, USA). FGF-R1 or PDGF-R mRNA was quantitated by real-time PCR as described in the supplementary information.

PCR analysis of immunoprecipitated DNA. Chromatin immunoprecipitation was performed following the Upstate Biotechnology ChIP kit protocol. U251MG cells were transduced with AAV vector at 1×10^4 genome copies/cell, pCMV-EGFP, or pAAV2EGFP in the presence or absence of the 1 ng/ml FR901228. Twenty-four hours after the transduction, chromatin proteins of interest were cross-linked to DNA. After preclearing, isotype-antibody control or anti-acetylated histone H3 or anti-histone H3 antibody (Upstate Biotechnology) was added to the sonicated chromatin solution and incubated overnight at 4°C with agitation. Resulting immune complexes were collected by the salmon sperm DNA–protein A agarose slurry. The eluted samples were treated with proteinase K and purified by phenol/chloroform extraction. Precipitated DNAs were analyzed for the vector-derived promoter by quantitative PCR with an ABI Prism 7700 sequence detection system as described in the supplementary information.

In vivo analysis of enhanced transgene expression. U251MG cells were treated with PBS ($n = 3$) or transduced with a recombinant AAV2 expressing luciferase (AAV2Luc) at 1×10^4 genome copies/cell for 1 h ($n = 5$), and then 3×10^6 of the transduced cells in 100 μl PBS containing 25% (v/v) basement membrane matrix (Matrigel; BD Biosciences, Franklin Lakes, NJ, USA) were inoculated subcutaneously into male BALB/c *nu/nu* mice (Clea Japan, Tokyo, Japan) along with intraperitoneal injection of FR901228 at 1 mg/kg or the same volume of vehicle. Twenty-four hours after the administration of FR901228, optical bioluminescence imaging was performed using the CCD camera (Xenogen Corp., Alameda, CA, USA). After intraperitoneal injection of reporter substrate D-luciferin (375 mg/kg body wt), mice were imaged for scans.

To analyze the effect of FR901228 on the enhanced tumor elimination *in vivo*, 9L tumor cells were transduced with an AAV5TK at 1×10^4 genome copies/cell for 1 h, and then 3×10^6 of the transduced cells in 100 μl PBS containing 25% (v/v) Matrigel were inoculated subcutaneously into BALB/c mice. The tumor-bearing animals received an intraperitoneal injection of FR901228 at 3 mg/kg (group 1, $n = 6$; group 3, $n = 10$) or PBS (group 2, $n = 6$). The animals were also exposed to ganciclovir at 100 mg/kg per day (groups 2 and 3) or PBS (group 1) for 14 consecutive days by intraperitoneal placement of the miniosmotic pumps (Alzet, Palo Alto, CA, USA) according to the manufacturer's instructions. Tumor growth was monitored two to three times a week by measuring two perpendicular tumor diameters using calipers and the volumes were calculated as $a \times b^2 \times 0.5$, where a is the length and b is the width of the tumor in millimeters. Animals with tumors larger than 2 cm in diameter were euthanized.

ACKNOWLEDGMENTS

FR901228 and FR901464 were kindly provided by Fujisawa Pharmaceutical Co., Ltd. We thank Avigen, Inc. (Alameda, CA, USA) for providing pAAV2H (identical to pHLP19) and pAdeno. We are also indebted to Dr. John A. Chiorini for providing pAAV5H (identical to 5RepCapB) and pAAV5RNL. We also thank Ms. Miyoko Mitsu for her encouragement and support. This study was supported in part by (1) grants from the Ministry of Health, Labor, and Welfare of Japan, (2) Grants-in-Aid for Scientific Research, (3) a grant from the 21st Century COE Program, and (4) the "High-Tech Research Center" Project for Private Universities, matching fund subsidy, from the Ministry of Education, Culture, Sports, Science, and Technology of Japan.

RECEIVED FOR PUBLICATION SEPTEMBER 20, 2005; REVISED OCTOBER 25, 2005; ACCEPTED NOVEMBER 19, 2005.

APPENDIX A. SUPPLEMENTARY DATA

Supplementary data associated with this article can be found in the online version at doi:10.1016/j.ymthe.2005.11.010.

REFERENCES

1. Carter, B. J. (2004). Adeno-associated virus and the development of adeno-associated virus vectors: a historical perspective. *Mol. Ther.* **10:** 981–989.
2. Okada, T., *et al.* (2002). Adeno-associated virus vectors for gene transfer to the brain. *Methods* **28:** 237–247.
3. Zaiss, A. K., Liu, Q., Bowen, G. P., Wong, N. C., Bartlett, J. S., and Muruve, D. A. (2002). Differential activation of innate immune responses by adenovirus and adeno-associated virus vectors. *J. Virol.* **76:** 4580–4590.
4. Kanazawa, T., *et al.* (2001). Gamma-rays enhance rAAV-mediated transgene expression and cytocidal effect of AAV-HSVtk/ganciclovir on cancer cells. *Cancer Gene Ther.* **8:** 99–106.
5. Kanazawa, T., *et al.* (2003). Suicide gene therapy using AAV-HSVtk/ganciclovir in

Copyright © The American Society of Gene Therapy

combination with irradiation results in regression of human head and neck cancer xenografts in nude mice. *Gene Ther.* **10:** 51–58.
6. Kanazawa, T., *et al.* (2004). Topoisomerase inhibitors enhance the cytocidal effect of AAV-HSVtk/ganciclovir on head and neck cancer cells. *Int. J. Oncol.* **25:** 729–735.
7. Kitazono, M., Goldsmith, M. E., Aikou, T., Bates, S., and Fojo, T. (2001). Enhanced adenovirus transgene expression in malignant cells treated with the histone deacetylase inhibitor FR901228. *Cancer Res.* **61:** 6328–6330.
8. Chen, W. Y., Bailey, E. C., McCune, S. L., Dong, J. Y., and Townes, T. M. (1997). Reactivation of silenced, virally transduced genes by inhibitors of histone deacetylase. *Proc. Natl. Acad. Sci. USA* **94:** 5798–5803.
9. Nakai, H., Yant, S. R., Storm, T. A., Fuess, S., Meuse, L., and Kay, M. A. (2001). Extrachromosomal recombinant adeno-associated virus vector genomes are primarily responsible for stable liver transduction in vivo. *J. Virol.* **75:** 6969–6976.
10. Vanoosten, R. L., Moore, J. M., Ludwig, A. T., and Griffith, T. S. (2005). Depsipeptide (FR901228) enhances the cytotoxic activity of TRAIL by redistributing TRAIL receptor to membrane lipid rafts. *Mol. Ther.* **11:** 542–552.
11. Summerford, C., and Samulski, R. J. (1998). Membrane-associated heparan sulfate proteoglycan is a receptor for adeno-associated virus type 2 virions. *J. Virol.* **72:** 1438–1445.
12. Qing, K., Mah, C., Hansen, J., Zhou, S., Dwarki, V., and Srivastava, A. (1999). Human fibroblast growth factor receptor 1 is a co-receptor for infection by adeno-associated virus 2. *Nat. Med.* **5:** 71–77.
13. Walters, R. W., *et al.* (2001). Binding of adeno-associated virus type 5 to 2,3-linked sialic acid is required for gene transfer. *J. Biol. Chem.* **276:** 20610–20616.
14. Di Pasquale, G., *et al.* (2003). Identification of PDGFR as a receptor for AAV-5 transduction. *Nat. Med.* **9:** 1306–1312.
15. Okada, T., *et al.* (2001). Development and characterization of an antisense-mediated prepackaging cell line for adeno-associated virus vector production. *Biochem. Biophys. Res. Commun.* **288:** 62–68.
16. Chiorini, J. A., Kim, F., Yang, L., and Kotin, R. M. (1999). Cloning and characterization of adeno-associated virus type 5. *J. Virol.* **73:** 1309–1319.
17. Okada, T., *et al.* (1997). Inhibition of gene expression from the human c-erbB gene promoter by a retroviral vector expressing anti-gene RNA. *Biochem. Biophys. Res. Commun.* **240:** 203–207.
18. Okada, T., *et al.* (2001). AV.TK-mediated killing of subcutaneous tumors in situ results in effective immunization against established secondary intracranial tumor deposits. *Gene Ther.* **8:** 1315–1322.
19. Okada, T., *et al.* (2002). Adeno-associated viral vector-mediated gene therapy of ischemia-induced neuronal death. *Methods Enzymol.* **346:** 378–393.
20. Okada, T., *et al.* (2005). Large-scale production of recombinant viruses using a large culture vessel with active gassing. *Hum. Gene Ther.* **16:** 1212–1218.
21. Nakajima, H., Kim, Y. B., Terano, H., Yoshida, M., and Horinouchi, S. (1998). FR901228, a potent antitumor antibiotic, is a novel histone deacetylase inhibitor. *Exp. Cell Res.* **241:** 126–133.
22. Sandor, V., *et al.* (2002). Phase I trial of the histone deacetylase inhibitor, depsipeptide (FR901228, NSC 630176), in patients with refractory neoplasms. *Clin. Cancer Res.* **8:** 718–728.

Copyright © The American Society of Gene Therapy

JOURNAL OF VIROLOGY, Feb. 2006, p. 1874–1885
0022-538X/06/$08.00+0 doi:10.1128/JVI.80.4.1874–1885.2006
Copyright © 2006, American Society for Microbiology. All Rights Reserved.
Vol. 80, No. 4

Scalable Generation of High-Titer Recombinant Adeno-Associated Virus Type 5 in Insect Cells

Masashi Urabe,[1]* Takayo Nakakura,[1] Ke-Qin Xin,[2] Yoko Obara,[1] Hiroaki Mizukami,[1] Akihiro Kume,[1] Robert M. Kotin,[3] and Keiya Ozawa[1]

Division of Genetic Therapeutics, Jichi Medical School, Tochigi 329-0498, Japan[1]; Department of Molecular Biodefense Research, Yokohama City University Graduate School of Medicine, Yokohama 236-0004, Japan[2]; and Laboratory of Biochemical Genetics, National Heart, Lung, and Blood Institute, National Institutes of Health, Bethesda, Maryland[3]

Received 14 June 2005/Accepted 27 November 2005

We established a method for production of recombinant adeno-associated virus type 5 (rAAV5) in insect cells by use of baculovirus expression vectors. One baculovirus harbors a transgene between the inverted terminal repeat sequences of type 5, and the second expresses Rep78 and Rep52. Interestingly, the replacement of type 5 Rep52 with type 1 Rep52 generated four times more rAAV5 particles. We replaced the N-terminal portion of type 5 VP1 with the equivalent portion of type 2 to generate infectious AAV5 particles. The rAAV5 with the modified VP1 required α2-3 sialic acid for transduction, as revealed by a competition experiment with an analog of α2-3 sialic acid. rAAV5-GFP/Neo with a 4.4-kb vector genome produced in HEK293 cells or Sf9 cells transduced COS cells with similar efficiencies. Surprisingly, Sf9-produced humanized *Renilla* green fluorescent protein (hGFP) vector with a 2.4-kb vector genome induced stronger GFP expression than the 293-produced one. Transduction of murine skeletal muscles with Sf9-generated rAAV5 with a 3.4-kb vector genome carrying a human secreted alkaline phosphatase (SEAP) expression cassette induced levels of SEAP more than 30 times higher than those for 293-produced vector 1 week after injection. Analysis of virion DNA revealed that in addition to a 2.4- or 3.4-kb single-stranded vector genome, Sf9-rAAV5 had more-abundant forms of approximately 4.7 kb, which appeared to correspond to the monomer duplex form of hGFP vector or truncated monomer duplex SEAP vector DNA. These results indicated that rAAV5 can be generated in insect cells, although the difference in incorporated virion DNA may induce different expression patterns of the transgene.

Recombinant adeno-associated virus (rAAV) is being developed as a gene transfer vector. rAAV based on serotype 2 (rAAV2) successfully transduces nondividing cells, including muscle, liver, and brain cells (29). Conventional rAAV production requires packaging of rAAV DNA into type 2 capsids by transient transfection of HEK293 cells with two or three plasmids: an AAV helper plasmid encoding *rep* and *cap* genes devoid of inverted terminal repeat (ITR) sequences, a vector plasmid harboring the therapeutic gene between ITRs, and an adenovirus helper plasmid expressing E2A, virus-associated (VA) RNA, and E4orf6. Transient cotransfection is the major limitation for scale-up of rAAV production. Since rAAV can be purified using column chromatography, which can result in highly purified rAAV while eliminating other contaminating viruses, some efforts were made to develop rAAV production systems by using recombinant mammalian viruses such as adenovirus (10) or herpes virus (4) which do not rely on the plasmid transfection and therefore may be amenable to scale-up production.

Recombinant baculoviruses based on the *Autographa californica* nuclear polyhedrosis virus are widely employed for production of heterologous proteins in cultured insect cells. The highly active, late *A. californica* nuclear polyhedrosis virus promoters, such as polyhedrin and p10 promoters, regulate the expression of heterologous proteins, resulting in large amounts of foreign proteins. Insect cells may be grown in suspension cultures in volumes ranging from shake flasks of sizes from, e.g., 50 to 400 ml, up to commercial-size bioreactors, e.g., 1,000 liters and larger. Recently, we described a highly scalable and efficient method for packaging rAAV2 in insect cells by use of baculovirus expression vectors (31). The ease of scale-up production is perhaps the most attractive feature of this production system. Infection of insect cells in suspension culture with recombinant baculoviruses eliminates the transfection process. Standard downstream processing to recover rAAV, such as tangential flow filtration and column chromatography, is readily applied.

In addition to vectors derived from serotype 2, other serotypes, utilizing different cell surface receptors, constitute a vector set from which an appropriate vector can be selected for a specific application. AAV5 is the most divergent dependovirus characterized (2), and type 5 AAV vectors have desirable properties that differ from other serotype vectors. AAV5 utilizes different receptors from other serotypes (14, 30), and rAAV5 has demonstrated different tropism from AAV2 (5), thus making it worthwhile to establish a method to produce rAAV5 in insect cells.

AAV is a member of the family *Parvoviridae*. The genome of AAV is a linear, single-stranded DNA of 4.7 kb in length. The ITRs flank the unique coding sequences for the nonstructural replication initiator proteins, Rep, and the structural capsid proteins, VP. The ITRs serve as origins of DNA replication and may also function as the packaging signal. Type 2 Rep78 is generated by the p5 promoter, while Rep68 is translated from spliced mRNA from the p5 promoter. The small Rep polypep-

* Corresponding author. Mailing address: Division of Genetic Therapeutics, Jichi Medical School, 3311-1 Yakushiji, Minami-kawachi, Tochigi 329-0498, Japan. Phone: 81-285-58-7402. Fax: 81-285-44-8675. E-mail: murabe@jichi.ac.jp.

tides Rep52 and Rep40 are expressed by the p19 promoter with nonspliced or spliced mRNA. The p40 promoter regulates expression of capsid proteins VP1, VP2, and VP3. Alternate usage of two splice sites and translation of VP2 at a non-AUG codon results in a stoichiometry of 1:1:10 of VP1, VP2, and VP3. Both p5 proteins Rep78 and Rep68 are AAV origin binding proteins, and the presence of either is required for AAV DNA replication and processing replicative intermediates of the virus DNA (13). Also, either Rep52 or Rep40 is necessary for packaging the single-stranded, linear virion genome into preformed empty capsids (17). The transcriptional map of type 5 AAV differs from that of type 2; the p7 promoter or p19 promoter transcribes mRNA for Rep78 or Rep52. Type 5 AAV does not encode the spliced form of Rep polypeptides Rep68 and Rep40 (25). Structural protein VP1 is a minor constituent in the AAV capsid. But the VP1-unique portion of approximately 140 amino acid residues is highly conserved among different serotypes and has a phospholipase A_2 motif. The YXGGX and HDXXY motifs (where X is any amino acid residue) in phospholipase A_2 indicate the catalytic site and Ca^{2+} binding loop, respectively (see Fig. 3A). Enzymes classified into the secretory phospholipase A_2 family hydrolyze the ester bond at the 2-acyl ester position of glycerophospholipids in the presence of Ca^{2+} and are involved in many aspects of cellular pathways, such as lipid membrane metabolism and signal transduction pathways (1, 21). The VP1-unique portion of parvovirus is required for transfer of the virus from late endosomes to the nucleus (36). A mutant virus lacking the VP1-unique portion or the activity of phospholipase is not processed properly, and thus no virus or vector genes are expressed.

In the present study, we describe a rAAV5 production system based on recombinant baculovirus and insect cells. In order to achieve high production levels of rAAV5 particles, we replaced a portion of the VP1 polypeptide with the corresponding portion of type 2. The VP1 substitution did not alter the tropism of rAAV5, which behaved indistinguishably from rAAV5 with wild-type VP1. In an attempt to improve the yields of rAAV5 particles, we used type 1 Rep52 instead of type 5, which resulted in the production of more than 5×10^4 vector genomes (vg) per insect cell.

MATERIALS AND METHODS

Plasmid construction. A flow chart of plasmid construction is shown in Fig. 1. pSR485 is an AAV5 vector plasmid harboring green fluorescent protein (GFP) and neomycin (Neo) genes between the ITRs (27). NotI sites were introduced outside the GFP/Neo expression cassette by PCR amplification using primers 5′-GATCGTCGACGCGGCCGCTCTCAGTACAATCTGCTCTGATGCC and 5′-AGTCGTCGACGCGGCCGCCTGCAGGCATGCAAGCTTGTGAAAAA AATGC. The NotI sites (underlined) were introduced. The resulting 4-kb DNA fragment was inserted into the BglII-SalI (blunt) sites of pSR485 (pSR485α). pFB5GFP was constructed by insertion of the 4.8-kb PagI fragment from pSR485 into the Eco105III site of pFBHTΔ, which was derived from pFBHTb (Invitrogen, Carlsbad, CA) after removal of the polyhedrin promoter with BstZ17I and HindIII digestion. A humanized *Renilla* GFP (hGFP) gene was excised from phrGFPII-1 (Stratagene, La Jolla, CA) by treatment with BamHI and EcoRV and subcloned into an expression plasmid regulated by the cytomegalovirus (CMV) immediate-early promoter (pCMV). The resulting plasmid, pCMVh GFP, was treated with NotI to cut out the entire hGFP expression cassette, which was inserted into the corresponding site of pSR485α or pFB5GFP (pSR485hGFP or pFB5hGFP, respectively). A human secreted alkaline phosphatase (SEAP) gene was excised from pSEAP2-Basic (Clontech, Mountain View, CA) with NruI and SalI, and the resulting 1.8-kb fragment was blunt-ended and inserted into pCMV. The entire SEAP cassette was then excised with NotI and inserted into the corresponding site of pAAVGFP or pFBGFPR (31) between the type 2 ITRs (pAAVSEAP or pFBSEAP, respectively). The type 5 p5 Rep open reading frame (ORF) equivalent to type 2 Rep78 was PCR amplified from pAAV5-2 (2) by using primers 5′-GAAGAAGCGCGCGTATGAGTTCT CGCGAGACTTC and 5′-CGATTTACTGTTCTTTATTGGCATCGTCAA AATC and inserted into a cloning vector. The Rep ORF was cut out by NruI and BssHII, blunt-ended, and subcloned into the NotI site (blunt) of pBACΔIERep (31), which was then treated with BglII and ClaI and blunt-ended, and the resulting 2.1-kb fragment was inserted into the NotI-PstI (blunt) sites of pFBDΔ (pFBD5LR). pFBDΔ is a derivative of FastBac Dual (Invitrogen) generated by the removal of the polyhedrin and p10 promoters with NcoI and BamHI treatment. The small Rep ORF was cut out from pFBD5LR by partial digestion with Eco47III and SalI, and the resulting 1.3-kb fragment was blunt-ended and inserted into the StuI site of pFastBac Dual (pFBD5SR). pFBD5SR was then digested with BstZ17I and SalI and treated with T4 DNA polymerase, and the resulting 1.4-kb fragment was inserted into the KpnI site (blunt) of pFBD5LR (pFBD5LSR). To generate the truncated p10 promoter, complementary 5′-phosphorylated oligonucleotides 5′-TAAAATCGCGAC and 5′-CATGGTCGC GATTTTAAT were annealed to each other and inserted into the PacI-NcoI sites of pFastBac Dual (pΔ5FBD). The type 5 Rep78 gene was PCR amplified with primers 5′-GCGCTTAATTAAAATCGCTAGTATGGCTACCTTCTATGA AGTCATT-3′ and 5′-GATCGCTAGCTTACTGTTCTTTATTGGCATCGT CA-3′ and subsequently digested with PacI and NheI and inserted into the PacI-NheI sites of pΔ5FBD (pFBD5LR12) (the Rep78 ORF is capitalized)). The type 5 Rep52 gene amplified using primers 5′-GATCGCGCGCCATGGCGCTCG TCAACTGGCTCGTGGAG-3′ and 5′-GATCGTCGACTTACTGTTCTTTAT TGGCATCGTCA-3′ was digested with BssHII and SalI and inserted into the corresponding sites of pFBD5LR12 (pFBD5LSR12α). To replace type 5 Rep52 on pFBD5LSR12α with type 1, 2, 3, or 4 Rep52, PCR was conducted with sense primer 5′-gatcccATGGAGCTGGTCGGGTGGCTGGTGGA-3′ and antisense primer 5′-gatcactagtTTATTGCTCAGAAACACAGTCATCCA-3′ (for type 1 or 3) or 5′-gatcactagtTTATTGTTCCATGTCACAGTCATCCA-3′ (for type 4) from AAV1 (purchased from American Type Culture Collection), an AAV2 helper plasmid pHLP19 (20), p3-2 (22), or p4-2 (3) (NcoI and SpeI sites are underlined). The resulting 1.2-kb DNA was digested with NcoI and SpeI and inserted into the corresponding sites of pFBD5LSR12α (pFBD5LSR121, pFBD5LSR122, pFBD5LSR123, and pFBD5LSR124). The resulting recombinant baculoviruses expressing type 5 Rep78 and type 1, 2, 3, 4, or 5 Rep52 are designated Rep5/1, 5/2, 5/3, 5/4, and 5/5, respectively. The type 5 VP ORF was obtained by PCR amplification from pAAV5-2 by using primers 5′-gtcaagcttcct gttaagACGTCTTTTGTTGATCACCCTCCAGATTGGT-3′ and 5′-cgaatctagaTT AAAGGGGTCGGGTAAGGTATCG-3′. The sequence corresponding to the VP ORF is capitalized, and the initiation codon was mutated to ACG to reduce its translational efficiency. The 2.2-kb PCR product was cloned into pCMV (pCMV5VPm). The plasmid was digested with Acc65I and treated with T4 DNA polymerase and subsequently with XbaI to excise the VP ORF, which was then inserted into the BamHI (blunt)-XbaI sites of pFastBac Dual (pFBD5VPm). Plasmid expressing a chimeric VP was constructed by the use of an overlapping-PCR method as follows. VP251 was generated by PCR from pAAV5-2 using primers #30 and #31 (Table 1). The resulting PCR product was treated with BamHI and HindIII and cloned into the corresponding sites of pFBD5VPm. For VP252 construction, the type 2 VP portion was PCR amplified with primers #32 and #34 from pHLP19. The type 5 VP was amplified with primers #33 and #31. After gel purification, the two PCR products were combined and subjected to the second round of PCR using primers #31 and #32. Chimeric VP253, -254, -255, and -256 were produced in the same way except for primers for the first round of PCR. For VP253, primers #32 and #36 were used to amplify the type 2 VP1 portion and #31 and #35 to amplify the type 5 VP portion (see Fig. 3A). A PCR-generated chimeric VP1 gene was digested with HindIII and BamHI and inserted into the HindIII-BamHI sites of pFBD5VPm.

Cell culture. HEK293 cells were maintained in Dulbecco's modified Eagle's medium–F-12 (1:1, vol/vol; Invitrogen) supplemented with 10% fetal calf serum (Sigma-Aldrich, St. Louis, MO). *Spodoptera frugiperda* Sf9 cells (Invitrogen) were grown at 27°C in shake flask cultures containing Sf-900 II SFM (Invitrogen) supplemented with 10% fetal calf serum.

Western blotting and silver staining. Cells were lysed in 1× sodium dodecyl sulfate sample buffer and resolved on a 4 to 12% NuPAGE Bis-Tris gel (Invitrogen). After electrophoresis, separated proteins were transferred to a Durapore membrane filter (Millipore, Bedford, MA) and incubated with a primary antibody, either an anti-Rep monoclonal antibody (303.9; Research Diagnostics, Flanders, NJ) at a dilution of 1:200 or a polyclonal anti-type 5 VP antibody raised against a portion of type 5 VP3 polypeptide at a dilution of 1:50,000. The blots

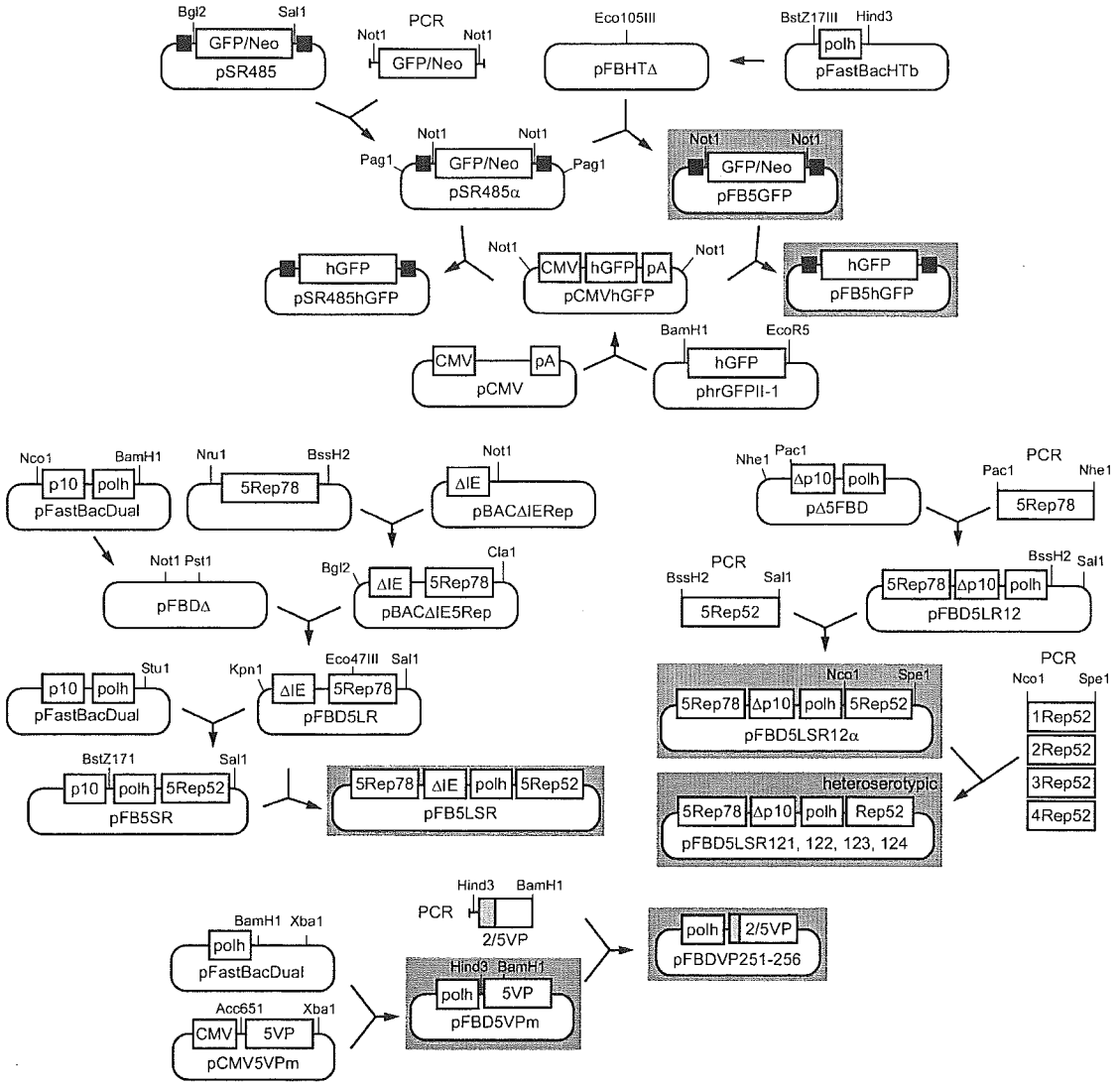

FIG. 1. Flow chart of plasmid construction. See Materials and Methods for details. Plasmids on gray backgrounds were used for generation of recombinant baculovirus vectors. Black boxes, type 5 ITR sequence; p10, p10 promoter; polh, polyhedrin promoter; pA, simian virus 40 polyadenylation sequence.

were then incubated with a secondary anti-mouse or anti-rabbit immunoglobulin G labeled with horseradish peroxidase at a dilution of 1:7,500 (Pierce, Milwaukee, WI). Membranes were incubated in Tris-buffered saline with Tween 20 (TBS-T) (10 mM Tris-HCl [pH 7.6], 0.15 M NaCl, 0.05% Tween 20, 5% nonfat dry milk). Antibodies were added to TBS-T for 1 h. After incubation, membranes were washed three times for 10 min each in TBS-T. All steps were performed at ambient temperature. The development of chemiluminescence catalyzed by horseradish peroxidase was performed according to the manufacturer's instructions (SuperSignal West Pico chemiluminescent substrate; Pierce), and the signals were detected with an X-ray film. Silver staining was performed using a SilverQuest silver staining kit (Invitrogen) according to the manufacturer's instructions.

Analysis of replicated rAAV DNA in Sf9 cells. Sf9 cells (2×10^5 cells per well) in 12-well plates were infected with GFP with or without Rep baculoviruses at a multiplicity of infection (MOI) of 3 and incubated at 27°C for 3 days. After incubation, extrachromosomal DNA was isolated by the method of Hirt (12) and a volume corresponding to 2×10^4 cells was resolved on a 0.8% agarose gel in Tris-borate buffer. Ethidium-stained gel was visualized under UV.

Production of rAAV5 in HEK293 cells. To produce rAAV5-GFP in mammalian cells, HEK293 cells at 80% confluence (approximately 10^5 cells per cm^2) in a 225-cm^2 flask were cotransfected with 27 μg of an AAV vector plasmid and 53 μg pSR487 by the calcium phosphate coprecipitation method. pSR487 harbors type 5 *rep* and *cap* genes and adenovirus E2A, E4orf6, and VA genes (27). Two days after transfection, rAAV5 was purified as described below. For production of pseudotyped type 5 rAAV-SEAP, HEK293 cells were cotransfected with pAAVSEAP; a Rep plasmid expressing type 2 Rep78, Rep68, Rep52, and Rep40; a VP plasmid expressing VP254; and an adenovirus helper plasmid.

Production and purification of rAAV5 in Sf9 cells. Typically, 4×10^8 Sf9 cells (2×10^6 cells per ml) were infected with a Rep baculovirus (RepBac), a VP baculovirus (VPBac), and a GFP baculovirus (GFPBac) with an MOI of 1 per baculovirus construct. To generate pseudotyped 2/5 rAAV-SEAP, Sf9 cells were infected with a RepBac expressing type 2 Rep78 and Rep52, VP254Bac, and SEAPBac. Pseudotype virus refers to the ITRs of one serotype packaged into a capsid derived from a different AAV serotype. For example, rAAV2/5 consists of AAV2 ITRs packaged into an AAV5 capsid. Three days after infection, the cells were pelleted by centrifugation and lysed in a lysis buffer of 20 mM Tris-HCl (pH 8.4), 50 mM NaCl, 2 mM $MgCl_2$, 0.4% deoxycholic acid, 0.5% 3-[(cholamidopropyl)-dimethylammonio]-l-propanesulfonate (CHAPS) (Merck, Darmstadt, Germany), and 60 U per ml of Benzonase (Merck) and incubated at 37°C for 30 min. The concentration of NaCl in the cell lysate was adjusted to 150 mM and incubated for an additional 30 min. Solid CsCl was added to obtain a final density of 1.36 g/cm^3. After centrifugation at 36,000 rpm for 24 h at 21°C using an SW40 Ti rotor (Beckman, Fullerton, CA), fractions containing rAAV5 were recovered and subjected to a second round of CsCl ultracentrifugation. For some experi-

TABLE 1. Oligonucleotides used for construction of chimeric VP genes

Primer	Sequence[a]
#30	5′-gtcaaagcttcctgttaagAcGGCTGCCGAcGGTTATCTaCCcGA TTGGTTGGAAGAAGTTGGTGAAGGT-3′
#31	5′-GCTGGGATCCGCTGGGTCCAGCTTCGGCGT-3′
#32	5′-gtcaaagcttcctgttaagAcGGCTGCCGAcGGTTATCTaCCcGA TTGGTTGGAGGAC-3′
#33	5′-ACAGCAGGGGTCTTGTGCTGCCTGGTTATAACTA-3′
#34	5′-TAGTTATAACCAGGCAGCACAAGACCCCTGCTGT-3′
#35	5′-GACTCGACAAGGGAGAGCCTGTCAACAGGGCAGA-3′
#36	5′-TCTGCCCTGTTGACAGGCTCTCCCTTGTCGAGTC-3′
#37	5′-GAGACAACCCGTACCTCAAGTACAACCACGCGGA-3′
#38	5′-TCCGCGTGGTTGTACTTGAGGTACGGGTTGTCTC-3′
#39	5′-GAGCAGTCTTCCAGGCGAAGAAAAGGGTTCTCGA-3′
#40	5′-TCGAGAACCCTTTTCTTCGCCTGGAAGACTGCTC-3′
#41	5′-AGGAACCTGTTAAGACGGCCCCTACCGGAAAGCG-3′
#42	5′-CGCTTTCCGGTAGGGGCCGTCTTAACAGGTTCCT-3′

[a] The HindIII or BamHI sites are underlined. The initiation codon for the VP1 gene was mutated to ACG. The possible splicing donor site was destroyed by introducing silent mutations. The VP ORFs are capitalized, and mutated nucleotides are indicated by lowercase letters.

ments, rAAV5 was further purified by anion-exchange column chromatography. CsCl-banded rAAV5 fractions were dialyzed against a buffer of 20 mM Tris-HCl (pH 8.4), 20 mM NaCl, 2 mM $MgCl_2$, and 4% glycerol and loaded onto a HiTrap Q Sepharose XL column (1-ml bed volume; Amersham Biosciences, Piscataway, NJ). Bound rAAV5 was eluted with a 20 to 500 mM linear NaCl gradient. Fractions containing rAAV5 were dialyzed against a buffer of 50 mM HEPES (pH 7.4), 150 mM NaCl, 2 mM $MgCl_2$, and 5% sorbitol and stored at −80°C until use. The titer of rAAV was determined by real-time PCR with CMV-specific primers 5′-TATGGAGTTCCGCGTTACATAACTTACGGT-3′ and 5′-GAC TAATACGTAGATGTACTGCCAAGTAGG-3′ on an HT7000 genetic analyzer (Applied Biosystems, Foster City, CA). Dilutions of pSR485 were employed as a copy number standard.

Competition experiment with a type 2 or type 5 AAV receptor analog. COS cells were plated in a 12-well plate at 30% confluence 24 h prior to infection. rAAV2-GFP or rAAV5-GFP was incubated in 0 or 20 μg per ml of heparin (Sigma-Aldrich), an analog of heparan sulfate proteoglycan (HSPG), for 2 h at room temperature. The cells were infected with adenovirus (3 PFU per cell) at 37°C for 2 h. The cells were washed with medium and then infected with rAAV2-GFP at 10^4 vg per cell or rAAV5-GFP at 10^5 vg per cell. At 24 h postinfection, the cells were visually examined under a fluorescent microscope and the percentages of positive cells were determined by flow cytometric analysis of 10^5 infected cells. Experiments were performed in triplicate. Competition experiments with α2-3 sialic acid were performed as described previously (14). COS cells were plated at 30% confluence 1 day before infection in a 12-well plate. The cells were infected with adenovirus (3 PFU per cell) and incubated at 37°C for 2 h. The adenovirus-containing medium was removed, and the cells were washed with medium. The cells were then infected with rAAV2-GFP (10^4 vg per cell) or rAAV5-GFP (10^5 vg per cell) for 1.5 h in 0 or 0.5 mM 3′-*N*-acetylneuraminyl-*N*-acetyllactosamine (3′-SLN) (Sigma-Aldrich), an analog of α2-3 sialic acid. The cells were washed twice with medium and further incubated for 1 day. The cells were then examined for GFP fluorescence, and the number of positive cells was measured by flow cytometry.

Treatment of cells with neuraminidase. COS cells were infected with adenovirus at 3 PFU per cell for 1 h at 37°C. The cells were treated with 0.08 U per ml of neuraminidase (*Vibrio cholerae*, type III; Sigma-Aldrich) for 1 h and infected with rAAV2-GFP at 10^4 vg per cell or rAAV5-GFP at 10^5 vg per cell for 2 h. The infected cells were then washed twice with medium and incubated for 1 additional day. The GFP-positive cells were counted by flow cytometry. Experiments were done in triplicate.

Muscle injection of rAAV5 in mice. A total of 10^{11} vg of pseudotyped rAAV5-SEAP produced in either 293 cells or Sf9 cells were injected into murine tibialis anterior muscles and blood was taken at the indicated weeks after injection. The serum SEAP activity was measured by a SEAP report gene assay (Roche Diagnostics, GmbH, Penzberg, Germany). The mouse study was approved by a review board at Jichi Medical School.

RESULTS

Construction of recombinant VP and Rep baculoviruses. Production of rAAV2 in insect cells uses three baculovirus vectors providing the following: (i) genes for three AAV structural proteins that form the virus capsid (VP1, VP2, and VP3), (ii) two of the AAV nonstructural proteins for replication and encapsidation (Rep78 and Rep52), and (iii) AAV vector DNA consisting of the gene of interest flanked by the AAV origins of replication (ITRs). In the presence of the AAV nonstructural proteins, the AAV vector DNA is "rescued" from the baculovirus genome and replicates as AAV via the ITRs (31).

Similarly to AAV type 2, the type 5 capsid proteins VP1, VP2, and VP3 are synthesized from two spliced mRNAs arising from the p41 promoter (Fig. 2A) (25). One mRNA is translated into VP1, while another transcript encodes VP2 and VP3. The initiation codon for VP2 is ACG, which is poorly utilized, resulting in the ribosome scanning through to the VP3 initiation codon AUG. The alternate usage of two acceptor sites and the poor utilization of the ACG initiation codon for VP2 are responsible for the 1:1:10 stoichiometry of VP1, VP2, and VP3. As shown in our previous report, the type 2 VP gene with an AAV intron does not express all of the VP polypeptides in insect cells (31). Mutating the VP1 AUG initiation codon to ACG resulted in production of VP1, VP2, and VP3 with a stoichiometry of approximately 1:1:10 from a single transcript without alternate splicing (31). Based on our initial success with AAV2, we constructed a similar type 5 VP baculovirus (VP5Bac) that harbored a type 5 VP gene where the initiation codon for VP1 was changed to ACG (Fig. 2B). Although this VP5Bac was able to produce type 5 capsids into which type 5 AAV vector DNA was incorporated, VP1 was poorly expressed compared to that synthesized in 293 cells (Fig. 2C). The resulting rAAV5-GFP particles poorly transduced COS cells. The calculated ratio of vector genomes to transducing units for the Sf9 cell-produced rAAV5-GFP was 10 times higher than the ratio for the 293 cell-produced counterpart. The VP1 polypeptides have phospholipase A_2 activity and are critical for efficient transfer of the viral genome from late endosomes to the nucleus (36). The efficiency with which a scanning eukaryotic ribosome recognizes an AUG codon for translational initiation is dependent on the local sequence context of the codon. The sequence ACCAUGG is optimal for initiation (18). Residue G at +4 seems particularly important for translation from a non-AUG codon where the A of the AUG codon is defined as +1 (11). In type 2 VP1, the nucleotide at +4 is G while the corresponding nucleotide at +4 in type 5 is U. To increase the efficiency of translation from an ACG codon for type 5 VP1 in insect cells, we tested some VP1 mutants that introduced a G residue at +4. However, these mutants also failed to produce infectious type 5 AAV particles (data not shown). The VP1-unique portion is conserved well among different serotypes compared to the VP3 portion that constitutes the majority of the viral capsids and is responsible for receptor binding specificity. The type 5 VP1-unique portion is approximately 70% identical to the equivalent portion of type 2 (Fig. 3A), while the type 5 VP3 portion is 60% homologous to the equivalent portion of type 2 (2). Since we successfully produced rAAV2 that was as infectious as the 293 cell-produced one, we tested a series of chimeric capsids between types 2 and 5 in which a part of the type 5 VP1-unique portion was replaced by the corresponding portion of type 2 VP1. Figure 3A shows the chimeric VP1 genes constructed. Figure 3B shows the Western analysis of type 5 VP poly-

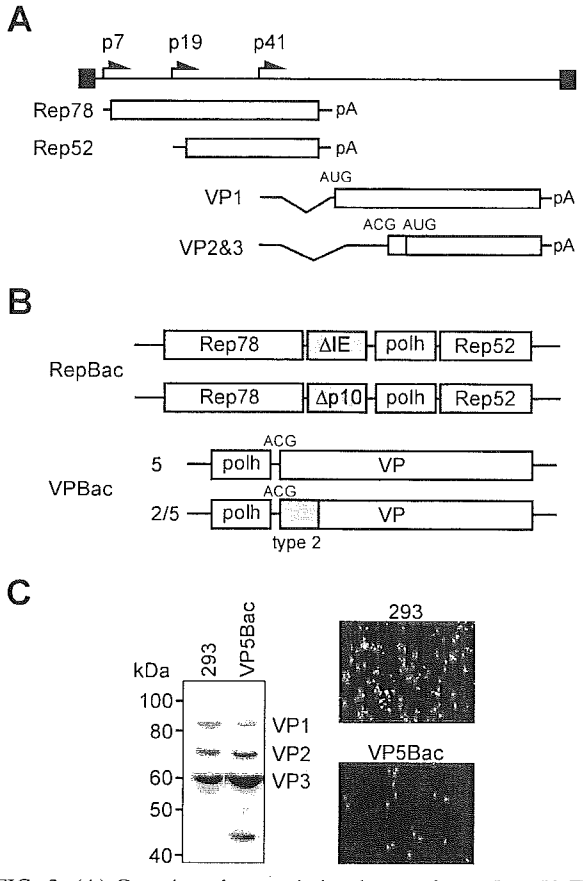

FIG. 2. (A) Genetic and transcriptional map of type 5 AAV. The p7 and p19 promoters drive Rep78 and Rep52, respectively. The p41 promoter transcribes two mRNAs. One expresses VP1, and the other is for VP2 and VP3. The initiation codon for VP2 is ACG, which is poorly utilized for translation, leading to production of a smaller amount of VP2 polypeptides than VP3 polypeptides. The ITRs are indicated by black boxes. pA, polyadenylation signal sequence. (B) Recombinant baculoviruses (rBac) constructed. An rBac for Rep utilizes a truncated promoter for the immediate-early 1 gene of *Orgyia pseudotsugata* nuclear polyhedrosis virus (ΔIE) for type 5 Rep78, and another RepBac expresses Rep78 under the control of a truncated p10 promoter (Δp10). See Fig. 4A for details. Either RepBac uses the polyhedrin promoter (polh) for Rep52. For expression of type 5 capsid proteins, a recombinant baculovirus that harbored a VP gene on which the initiation codon for VP1 is mutated to ACG was constructed (VP5Bac). Another series of VPBacs that had the type 5 VP1 gene partially replaced by the corresponding portion of type 2 VP1 at the N terminus was generated. (C) Western analysis of Sf9 cells infected with VP5Bac. The initiation codon for VP1 was mutated to an ACG codon, which enabled synthesis of VP1, -2, and -3 from a single VP mRNA. The amount of VP1 synthesized was extremely small compared to that in 293 cells. rAAV5-GFP generated with VP5Bac was used for the infection of COS cells at 10^5 vg per cell. The number of GFP-positive cells was 10% of the number of positive cells obtained with rAAV5-GFP produced in 293 cells.

peptides produced with VP251Bac through VP256Bac. Each VPBac produced chimeric VP1 at levels comparable to those of VP2. Formation of empty capsids was confirmed by CsCl density gradient analysis of Sf9 cell lysate infected with VP254Bac, as shown in Fig. 3C. The peak of VP polypeptides came to the fraction of 1.31 g/cm^3, a buoyant density of empty capsids. The GFP gene between the type 5 ITRs could be packaged into each type of chimeric capsid, and all of the chimeric rAAV5-GFPs except VP251 could transduce COS cells with efficiency similar to that of 293 cell-produced rAAV5-GFP (data not shown). The yields of rAAV5-GFP produced with VP253Bac or VP254Bac were approximately 1.2 times higher than others, although the difference was not statistically significant. We thus used VP254Bac to produce rAAV5 for the next experiments.

The initial Rep baculovirus for type 2 rAAV production drove type 2 Rep72 expression with a truncated promoter for the immediate-early 1 gene of *Orgyia pseudotsugata* nuclear polyhedrosis virus (ΔIE) and type 2 Rep52 under the control of the polyhedrin promoter (31) (Fig. 2B). The AAV5 genome encodes nonstructural proteins Rep78 and Rep52 (Fig. 2A). Similarly, we constructed a Rep baculovirus that expressed type 5 Rep78 and Rep52 under the control of the ΔIE promoter and the polyhedrin promoter, respectively. The titers of the type 2 or type 5 Rep baculoviruses, however, were lower than those of other recombinant baculovirus vectors (e.g., VPBac, GFPBac). The immediate-early 1 gene promoter becomes active at the early stage of baculovirus infection, and we thought that early expression of Rep78 in insect cells might negatively affect the yields of recombinant baculoviruses. The very late p10 promoter, which is widely used for recombinant protein production, is active at the latest stage of baculovirus infection. Thus, to delay and suppress the expression of Rep78, we tested a series of truncated p10 promoters. First, we screened the truncated p10 promoters for production of type 2 rAAV and selected one that generated high-titer rAAV2. Figure 4A shows the map of the p10 promoter and the truncated p10 promoter we constructed. The upstream TAAG sequence does not affect the activity of the p10 promoter (32). The sequence between the TAAG sequence and the p10 protein initiation codon at +72 (where the transcription start site is defined as +1) is called the burst sequence and is required for the "burst" of expression of the p10 protein at the very late stage of baculovirus infection. The *vlf-1* transactivator interacts with the burst sequence and strongly stimulates the transcription from the p10 promoter (35). To construct a weak p10 promoter (Δp10), we removed the burst sequence between positions +39 and +72 from the original p10 promoter. The Δp10 promoter was best for the production of rAAV2 among a series of truncated p10 promoters we examined. The titers of recombinant baculoviruses with the Δp10 promoter were comparable to those of other recombinant baculoviruses. The Δp10 promoter was transferred to express type 5 Rep78 (Fig. 2B). Figure 4B compares the time courses of type 5 Rep expression by ΔIE and Δp10 promoters over 72 h after infection, indicating that the Δp10 promoter-driven Rep78 expression was detected at 24 h after infection while the ΔIE promoter expressed Rep78 as early as 12 h after infection. To examine whether this modest difference in the levels of Rep78 affected replication of the AAV vector DNA, we isolated the low-molecular-weight DNA from the Sf9 cells infected with hGFP baculovirus and a Rep baculovirus (Fig. 4C). A ladder of replicative forms (RF) of rAAV5 DNA began to appear at 36 h postinfection in either case. The expected size of rAAV5-hGFP or monomer RF is 2.4 kb and the sizes of dimer and trimer RF are 4.8 and 7.2 kb, which is consistent with the result of the agarose gel electrophoresis.

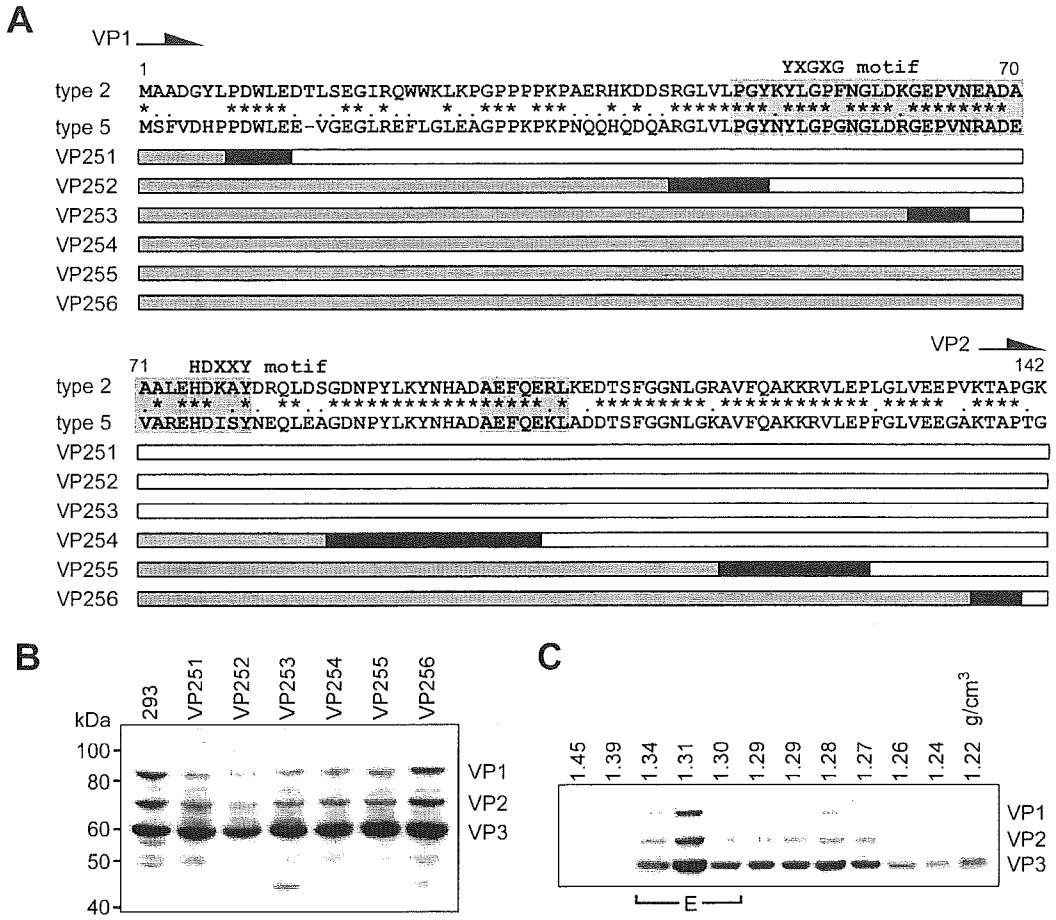

FIG. 3. (A) Chimeric VP genes constructed. The portions derived from type 2 are indicated in gray, while those from type 5 are in white. The common portions are indicated in black. The phospholipase A_2 motifs are shaded. The YXGGX and HDXXY motifs (where X is any amino acid residue), indicating the catalytic site and Ca^{2+} binding loop, respectively, are also shown. The amino acid residues common between type 2 and type 5 are indicated by asterisks. Amino acid residues classified into the same group are indicated by dots. (B) Expression of chimeric VP polypeptides in Sf9 cells. One microgram of cell lysate was resolved onto a 4 to 12% NuPAGE Bis-Tris gel in MOPS (morpholinepropanesulfonic acid) buffer (Invitrogen). Separated proteins were transferred to a Durapore membrane (Millipore), and VP proteins were detected with a rabbit polyclonal antibody raised against the type 5 VP3 portion. The lane labeled 293 shows lysate from HEK 293 cells transfected with pSR487, a hybrid plasmid harboring type 5 AAV *rep* and *cap* genes and adenovirus E2A, VA RNA, and E4orf6 genes (27). Lanes labeled VP251 through VP256 indicate lysates from Sf9 cells infected with recombinant baculovirus expressing chimeric VP. (C) Chimeric VP between types 2 and 5 is able to form empty particles. Sf9 cells (1×10^7 cells) infected with a VP2/5Bac, VP253Bac, were lysed as described in Materials and Methods. Solid CsCl was added to make a buoyant density of 1.30 g/cm^3. After ultracentrifugation for 24 h at 36,000 rpm at 21°C using an SW40 Ti rotor (Beckman), 1-ml fractionations were collected. A portion of each fraction was resolved onto a 4 to 12% NuPAGE gel in MOPS buffer, transferred to a Durapore membrane, and detected with a rabbit anti-type 5 VP polyclonal antibody. The buoyant density of each fraction is indicated above each lane. Fractions that contain empty capsids are indicated by E.

Heteroserotypic small Rep can package rAAV5 DNA into type 5 capsids. The insect cell-based production system for rAAV2 or rAAV1 can generate more than 4×10^4 particles of rAAV per Sf9 cell. However, the yields of rAAV5 produced with either ΔIE or Δp10 RepBac were approximately 1×10^4 to 2×10^4 vg per Sf9 cell. Rep52, or small Rep protein, has been implicated in encapsidation of the AAV genome (17). To establish a high-titer production system, we investigated the use of other serotypes of Rep52 for rAAV5 production. We replaced the type 5 Rep52 with serotype 1, 2, 3, or 4 Rep52 on the Δp10 RepBac. Figure 5A shows the results of Western blotting of Sf9 cells infected with Rep baculoviruses expressing type 5 Rep78 under the control of the Δp10 promoter and serotype 1, 2, 3, 4, or 5 Rep52 driven by the polyhedrin promoter. To generate rAAV5, Sf9 cells were coinfected with hGFPBac, VP254Bac, and a RepBac with the indicated serotype Rep52 at an MOI of 1. Sf9 cells infected with hGFPBac and VP254Bac along with RepBac producing type 1 Rep52 were processed by CsCl density centrifugation, and fractions were analyzed for capsid antigen by Western blotting (Fig. 5B). Two peaks of VP proteins were detected; the higher-buoyant-density peak, from 1.42 to 1.36 g/cm^3, presumably consists of a vector genome containing rAAV5 particles. Another peak, at 1.33 g/cm^3, represents empty capsids, indicating that type 1 Rep52 packaged serotype 5 rAAV DNA into type 5 capsids. When a RepBac that expressed only type 5 Rep78 was used, no rAAV5 particles were produced, confirming that heteroserotypic small Rep indeed packaged type 5 rAAV DNA into type 5 capsids. The cell lysate was loaded directly onto an anion-exchange column, and purified particles were investigated un-

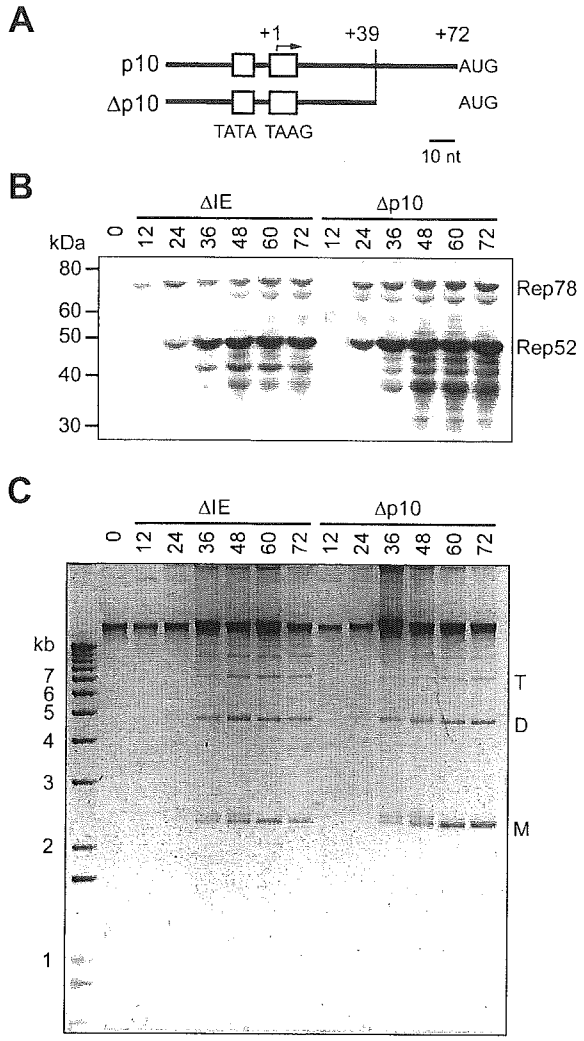

FIG. 4. (A) Map of the Δp10 promoter used for Rep78 expression. The sequence between positions +39 and +72 is deleted in the Δp10 promoter, where the T of the TAAG sequence or the transcription start site (marked with a bent arrow) is defined as +1 and the A of the p10 protein AUG codon is defined as +72. The original AUG codon for the p10 protein was mutated to ACT with pFastBac Dual (Invitrogen). The positions of the TATA box and the TAAG sequence are indicated. (B) Time course of Rep78 expression by ΔIE or Δp10 promoter. Sf9 cells were infected with a Rep baculovirus, and the cells were harvested at the times indicated (in hours) for Western analysis with a monoclonal anti-Rep antibody. (C) Replication of hGFP vector DNA in insect cells. Sf9 cells were coinfected with a Rep baculovirus and an hGFP baculovirus at 1 PFU per cell and incubated for the times indicated (in hours). Low-molecular-weight DNA was isolated, and DNA equivalent to 10^5 cells was resolved onto a 1% agarose gel. T, trimer replicative form; D, dimer; M, monomer.

der electron microscopy, showing typical rAAV particles of a diameter of 20 nm in addition to empty capsids (Fig. 5C). According to the staining pattern, approximately 30% of capsids contained vector genomes. In another experiment, rAAV5-hGFP was purified with two rounds of CsCl ultracentrifugation and the titers of rAAV5-hGFP were determined by real-time PCR using a pair of CMV-specific primers. Figure 5D summarizes the yields of rAAV5-hGFP with the use of different serotypes of small Rep. The titer of rAAV5-GFP produced with type 1, 2, 3, or 4 small Rep was 56,000 ± 3,200 (n = 4), 41,000 ± 18,900 (n = 4), 42,000 ± 7,300 (n = 3), or 39,000 ± 3,500 (n = 3) particles per Sf9 cell, respectively, while that of rAAV5-GFP produced using AAV5 Rep52 was 13,500 ± 3,200 (n = 5). The rAAV5-hGFP particles produced with the indicated serotype Rep52 were further purified by anion-exchange column chromatography, and a total of 3×10^9 vg of either rAAV5-hGFP were then fractionated by sodium dodecyl sulfate-polyacrylamide gel electrophoresis and examined by silver staining along with 293 cell-produced rAAV5-hGFP (Fig. 5E). Densitometric analysis indicated that the intensities of the VP3 bands were almost equal to one another.

Type 5 vector DNA was packaged into type 5 capsids consisting of chimeric VP1 between types 2 and 5 in the baculovirus system. To examine the possible effect of the chimeric VP1 on packaging of type 5 vector DNA with heteroserotypic Rep52, we tested the production of rAAV5-hGFP by using either Rep5/1Bac or Rep5/5Bac and VP5Bac or VP254Bac. Interestingly, the yields of rAAV5 produced with type 5 Rep52 and type 2/5 chimeric capsids were constantly lower than yields produced with other combinations (Fig. 5F). Type 1 Rep52 was capable of packaging type 5 vector DNA into type 5 capsids and type 2/5 chimeric capsids with similar levels of efficiency. Although the result was not conclusive, the presence of a type 2 VP1-unique portion might interfere with type 5 Rep52 packaging rAAV5 DNA into type 5 capsids in insect cells.

Insect cell-produced rAAV5 infects cells via an α2-3 sialic acid receptor. AAV2 capsids utilize HSPG as a primary coreceptor to infect target cells (30), whereas AAV5 capsids require α2-3 sialic acid for efficient uptake (14). rAAV5 capsids generated in Sf9 cells are composed of VP1 partially replaced with type 2 VP1. The domains involved in receptor binding are within the VP3 portion (16), and the type 2 VP1-unique portion does not appear to be involved in attachment to target cells (19). To determine whether rAAV5 chimeric capsid particles infect cells via sialic acid and not via HSPG, we performed competition experiments with receptor analogs. The results of the heparin competition study show that rAAV2-GFP failed to transduce COS cells in the presence of heparin, an analog of heparan sulfate, as expected (Fig. 6A, top panels). By contrast, rAAV5-GFP produced in 293 cells (Fig. 6A, middle panels) or insect cells (Fig. 6A, bottom panels) was able to express GFP in COS cells irrespective of the presence of heparin, suggesting that Sf9 cell-produced rAAV5-GFP did not utilize HSPG as a primary coreceptor. The number of GFP-expressing cells was counted by flow cytometry, and the percent change in transduction compared to transduction in the absence of heparin was calculated, which clearly corroborated the observation with fluorescent microscopy. We next examined whether insect cell-produced rAAV5-GFP infects cells via α2-3 sialic acid. As shown in Fig. 6B, COS cells were infected with rAAV5 generated in 293 cells (middle panels) or Sf9 cells (bottom panels) in the presence or absence of an analog of α2-3 sialic acid, 3′-SLN. The analog inhibited GFP expression in COS cells by both 293 cell- and Sf9 cell-produced rAAV5-GFP, suggesting that rAAV5-GFP produced in insect cells infected cells via α2-3 sialic acid as did 293 cell-produced rAAV5. To confirm that rAAV5-GFP derived from insect cells utilized sialic acid as a cell attachment receptor, we infected cells denuded of sialic acid by neuraminidase treatment. The

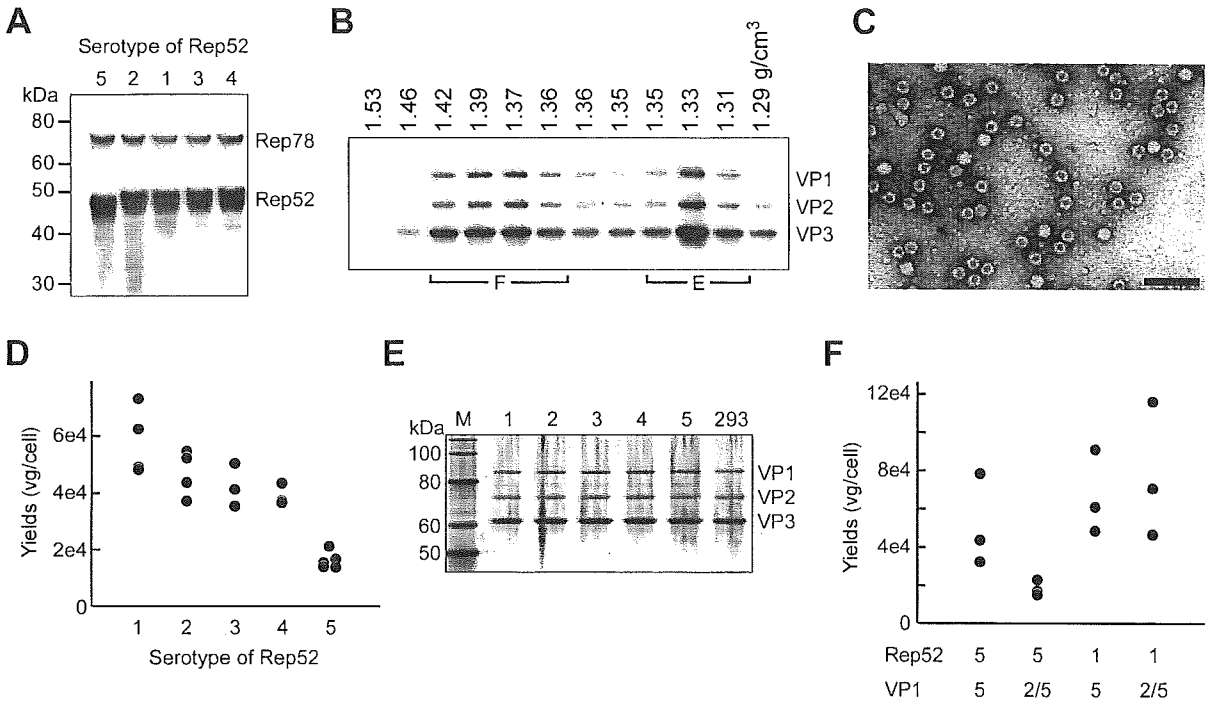

FIG. 5. (A) Western analysis of RepBacs expressing type 5 Rep78 and type 1, 2, 3, 4, or 5 Rep52 with an anti-Rep antibody. (B) Analysis of Sf9 cells coinfected with Rep, VP254, and hGFP baculoviruses by CsCl density gradient ultracentrifugation. Three days after infection, the cells were lysed and subjected to ultracentrifugation. F, filled, or containing rAAV particles; E, empty capsids. (C) Negative staining of rAAV5-hGFP particles purified with ion-exchange column chromatography alone. Particles were stained with 2% uranyl acetate. Magnification, ×100,000. Bar, 100 nm. (D) Generation of rAAV5-hGFP produced with different serotypes of Rep52. The yield of rAAV5-GFP produced with type 1, 2, 3, 4, or 5 small Rep was 56,000 ± 3,200 (n = 4), 41,000 ± 18,900 (n = 4), 42,000 ± 7,300 (n = 3), 39,000 ± 3,500 (n = 3), or 13,500 ± 3,200 (n = 5) particles per Sf9 cell, respectively. (E) Analysis of rAAV5-hGFP produced in insect cells or 293 cells by silver staining. rAAV5-hGFP (3×10^9 particles) produced with serotype 1, 2, 3, 4, or 5 and that produced in 293 cells were resolved onto a 4 to 12% NuPAGE Bis-Tris gel (Invitrogen). Lane M, molecular size markers. (F) Comparison of the yields of rAAV5-GFP produced with type 1 or type 5 Rep52 and VP5Bac or VP2/5Bac. Sf9 cells were coinfected with hGFPBac, Rep5/1Bac or Rep5/5Bac, and VP5Bac or VP254Bac at an MOI of 1 in each of three independent experiments. The rAAV5-hGFP produced was purified by two rounds of CsCl density gradient ultracentrifugation, and the genomic titer was determined by real-time PCR.

result shows that prior incubation with neuraminidase significantly inhibited the transduction of COS cells mediated by rAAV5-GFP produced in 293 cells and Sf9 cells (Fig. 6C).

Comparison of transduction efficiencies with rAAV5 in cultured cells. We next compared the efficacy of rAAV5-GFP/Neo produced in Sf9 cells to that for a mammalian-cell-produced counterpart. COS cells were infected with either Sf9-produced or 293-produced rAAV5-GFP/Neo at 1×10^5 through 1×10^2 vg per cell for 1 day, and the number of GFP-positive cells was counted by flow cytometry. As shown in Fig. 7A, both Sf9-produced and 293-produced rAAV5-GFP/Neo showed similar dose-response curves. In addition, the vector genome-to-transducing unit ratio was calculated based on the number of GFP-positive cells at 3×10^3 vg per cells. Three independently produced samples were examined, and the vector genome-to-transducing unit ratio for Sf9-produced rAAV5-GFP was $3.9 \times 10^4 \pm 1.6 \times 10^4$ (mean ± standard deviation), while the ratio for 293-produced rAAV was $3.6 \times 10^4 \pm 1.2 \times 10^4$. These results indicated that insect cell-generated rAAV5-GFP/Neo had a similar ability to transduce COS cells. Although the capsids produced in Sf9 cells contain type 2/5 chimeric VP1 and those produced in HEK293 cells were composed of original type 5 VP1, rAAV5-GFP/Neo derived from Sf9 cells and that derived from HEK293 cells did not show any significant difference in GFP expression in COS cells, suggesting that the difference in the VP1-unique portion did not impact the expression of the transgene or affect the intracellular processing of type 5 capsids in COS cells. We also compared transduction efficiencies of rAAV5-hGFP generated in Sf9 cells and rAAV5-hGFP generated in HEK293 cells. Surprisingly, the dose-response curve obtained by Sf9-produced rAAV5-hGFP shifted to the right and the number of GFP-positive cells at the dose of 3×10^3 vg per cell was five times larger than that for 293-produced rAAV5-hGFP (Fig. 7B). Since the substitution of the type 5 VP1-unique portion with the equivalent portion of type 2 did not impact the GFP expression in COS cells (Fig. 7A), we explored the rAAV genomes packaged into vector capsids. Virion DNA was isolated and analyzed on an alkaline gel. After electrophoresis, the DNA was transferred to a nylon membrane and hybridized with a ^{32}P-labeled CMV-specific probe. The GFP/Neo DNA packaged into AAV5 capsids is essentially the same in size and amount as expected (Fig. 7C). We next analyzed virion DNA isolated from rAAV5-hGFP produced with the indicated serotype Rep52 in insect cells, as well as 293-produced rAAV5-hGFP (Fig. 7D). The encapsidated hGFP DNA is present as